Title

Hyaluronan-CD44 interaction stimulates Rac1 signaling and PKN gamma kinase activation leading to cytoskeleton function and cell migration in astrocytes

Journal

Journal of Neurochemistry, 101

ISSN

0022-3042

Authors

Swanson, Raymond A.
Brightman, Amy
Bourguignon, Lilly Y. W.
et al.

Publication Date

2007-05-01

Peer reviewed

Hyaluronan-CD44 Interaction Stimulates Rac1 Signaling and PKNγ Kinase Activation Leading to Cytoskeleton Function and Cell Migration in Astrocytes

Lilly Y.W. Bourguignon[1]#, Eli Gilad[1], Karine Peyrollier[1], Amy Brightman[1] and Raymond Swanson[2]

Departments of Medicine[1] and Neurology[2], University of California San Francisco, Endocrine Unit (111N), San Francisco VA Medical Center, 4150 Clement Street, San Francisco, CA 94121.

#Reprint requests should be addressed to:

Dr. Lilly Y.W. Bourguignon
Endocrine Unit (111N),
Department of Medicine
University of California-San Francisco
and VA Medical Center
4150 Clement Street
San Francisco, CA 94121
TEL: (415) 221-4810 x 3321
FAX: (415) 383-1638
e-mail:Lilly.Bourguignon@ucsf.edu

Running Title: HA/CD44-mediated Rac1-PKNγ signaling in astrocytes.

Key Words: Hyaluronan, CD44, Rac1, PKNγ, Cytoskeleton, Astrocyte, Migration.

ABBREVIATIONS: HA, Hyaluronan; PKNγ, protein kinase N-γ; ACC, the antiparallel coiled-coil; F-actin, filamentous actin; CNS, central nervous system; PLCγ, phospholipase C-γ; PKC, protein kinase C.

ABSTRACT

Both hyaluronan [HA, the major glycosaminoglycans in the extracellular matrix (ECM)] and CD44 (a primary HA receptor) are associated with astrocyte activation and tissue repair following central nervous system (CNS) injury. In this study we investigated the question of whether HA-CD44 interaction influences astrocyte signaling and migration. Our data indicated that HA binding to the cultured astrocytes stimulated Rac1 signaling and cytoskeleton-mediated migration. To determine the cellular and molecular basis of these events, we focused on PKNγ, a Rac1-activated serine/threonine kinase in astrocytes. We determined that HA binding to astrocytes stimulated Rac1-dependent PKNγ kinase activity which, in turn, upregulated the phosphorylation of the cytoskeletal protein, cortactin, and attenuated the ability of cortactin to cross-link F-actin. Further analyses indicated that the N-terminal antiparallel coiled-coil (ACC) domains of PKNγ interacted with Rac1, and transfection of astrocytes with PKNγ-ACCcDNA inhibited PKNγ activity. Overexpression of the PKNγ-ACC domain also functions as a dominant-negative mutant to block HA/CD44-mediated PKNγ activation of cortactin and astrocyte migration. Taken together, these findings strongly suggest that hyaluronan/CD44 interaction with Rac1-PKNγ plays a pivotal role in cytoskeleton activation and astrocyte migration. These newly discovered HA/CD44-induced astrocyte function may provide important insight into novel therapeutic treatments for tissue repair following CNS injury.

INTRODUCTION

Astrocytes are the most abundant cells in the central nervous system (CNS) and traditionally are thought to be primarily neuron-supporting cells (Fitch and Silver, 2001; Barres and Barde, 2000). Evidence is now accumulating that astrocytes not only play an essential role in maintaining the homeostatic neuronal environment, but also participate in CNS pathogenesis due to trauma, viral/bacterial infections or chronic neurodegeneration (Haydon, 2000; Song, et al., 2002; Ullian, et al., 2001; Chen and Swanson, 2003). During CNS injury, a breakdown of the blood-brain barrier generally leads to reactive astrogliosis or glial scarring which involves

increased cell division, protein synthesis and cell migration of the astrocytes (Eddleston and Mucke, 1993; Ridet et al., 1997). Formation of a glial scar is considered to be one of the major obstacles to neuronal regeneration (Stichel and Muller, 1998; Nieto-Sampedro, 1999; David and Lacroix, 2003). Other cellular behaviors, including abnormal astrocyte migration to the site of injury to provide support for neuron regeneration and axonal regrowth (Rhodes et al., 2003; Silver and Miller, 2004), could also contribute to the poor ability of CNS to repair itself (Shearer and Fawcett, 2001; Sivron and Schwartz, 1995). Thus, understanding the cellular and molecular mechanisms involved in regulating astrocyte functions (in particular, cell migration) following CNS wounding/damage may be very useful for designing new therapeutic treatments for CNS repair.

Hyaluronan (HA) is one of the major glycosaminoglycans in the extracellular matrix (ECM) and plays an important role in morphogenesis, remodeling and integrity of the CNS (Asher et al., 1991; Bignami et al., 1992; Bignami and Asher, 1992; Eggli et al., 1992). It is synthesized by several HA synthases (Lee and Spicer, 2000; Toole, 2001) and modified by hyaluronidases (Tona and Bignami, 1993). Under physiological conditions, HA in these tissues exists as a large polymer in excess of 1 x 10^6 Da ("high molecular weight HA"). However, following CNS and other injuries, large HA becomes degraded (via hyaluronidases) into smaller HA units (1 x 10^4-1 x 10^3 Da; "low molecular weight HA") as reactive astrogliosis proceeds (Struve et al., 2005). In fact, injection of hyaluronidases into normal spinal cord tissue induces HA degradation and astrocyte proliferation (Struve et al., 2005). Both high and low molecular weight HAs are capable of binding to CD44 which is a ubiquitous, abundant and functionally important receptor expressed on the surface of many cells, including astrocytes (Underhill, 1992; Haegel et al., 1993). In uninjured CNS, the expression of CD44 is restricted to astrocytes in the white matter (Quackenbush, et al., 1985). However, upon CNS injury CD44 expression is upregulated at the injured sites (Jones et al., 2000). The question of whether HA-CD44 interaction actually plays an important role in regulating astrocyte function (e.g. migration)

following injury has not been carefully investigated; and thus is the focus of this study.

Several lines of evidence indicate that the actin cytoskeleton is directly involved in regulating astrocyte morphological changes and migration (Baorto et al., 1992; Ramakers and Moolenaar, 1998; Etienne-Manneville and Hall 2002; Holtje et al., 2005). Members of the Rho subclass of the Ras superfamily (small molecular weight GTPases, e.g. RhoA, Rac1 and Cdc42) are known to transduce incoming signals which result in the formation of cytoskeleton-mediated membrane protrusions and cell migration in many cell types including astrocytes (Hall, 1998). Overexpression of certain RhoGTPases in astrocytes occurs at the site of the CNS injury (Erschbamer et al., 2005). RhoGTPases have also been found to be involved in astrocytic wound closure following *in vitro* wounding using a scratch-wound assay (Etienne-Manneville and Hall 2002; Holtje et al., 2005). Specifically, RhoA has been shown to negatively regulate astrocyte morphology and migratory response after injury (Holtje et al., 2005). Other GTPases, such as Rac1, are also known to be key components in regulating actin cytoskeleton and cell migration (Hall, 1998). The question of whether Rac1 positively regulates cytoskeleton function and cell migration in astrocytes following wounding has not been addressed previously.

HA has been shown to activate CD44-mediated Rac1 signaling and cell migration in a variety of non-neuronal cell types (Bourguignon et al., 2000; Bourguignon et al., 2001a; Bourguignon et al., 2004). Furthermore, several enzymes have been identified as possible downstream targets for Rac1 signaling (Burbelo et al., 1995). One such enzyme is protein kinase N-γ (PKNγ) (also called PRK2 or PKN-2) which belongs to a family of serine-threonine kinases known to interact with Rac1 in a GTP-dependent manner and to share a great deal of sequence homology with protein kinase C (PKC) in the C-terminal region (Quilliam et al., 1996; Vincent and Settleman, 1997; Mukai, 2003). The N-terminal region of PKN contains three homologous stretches of approximately 70 amino acids (relatively rich in charged residues) that form the antiparallel coiled-coil fold (ACC domain) (Mukai, 2003; Vincent and Settleman, 1997; Quilliam et al., 1996; Yoshinaga et al., 1999). This ACC domain is known to interact with RhoGTPases

such as Rac1 (and to a lesser extent with RhoA or Cdc42) (Vincent and Settleman, 1997; Quilliam et al., 1996). The C-terminal region contains the C2-like region which functions as an auto-inhibitory domain (Yoshinaga et al., 1999). The ACC and the C2-like domains, together with the catalytic domain, are conserved among the PKN family members (Mukai, 2003). Most importantly, the ACC domain has been shown to interact with GTP-bound RhoGTPases such as Rac1 (Quilliam et al., 1996; Vincent and Settleman, 1997; Bourguignon, et al., 2004). Our recent work demonstrates that HA-CD44 interaction with Rac1-activated PKNγ promotes PLCγ1-regulated Ca^{2+} signaling and cortactin-cytoskeleton interaction required for a variety of cellular functions (Bourguignon et al., 2004). Although Rac1 has been closely associated with the remodeling of cortical actin, the Rac1-specific effector and its roles in regulating HA/CD44-mediated astrocyte functions have not been identified or characterized. In this study we have examined the role of HA/CD44-mediated Rac1-PKNγ kinase signaling and its downstream effectors in the regulation of astrocyte functions involving cytoskeleton activation and cell migration.

MATERIALS AND METHODS

Cell Cultures: Astrocyte cultures were prepared from cortices of one-day-old Swiss-Webster mice (Simonsen, Gilroy, CA) as described previously (Swanson et al., 1997) and maintained in Eagle's MEM containing 10% fetal bovine serum (FBS) and glutamine (2mM) in a humidified, 5% CO2 incubator at 37^{o}C. The medium were exchanged with fresh medium at day 5. At confluence (days 12-15), 10μM cytosine arabinoside were added to prevent proliferation of other cell types. This medium were removed after 48h, replaced with medium containing 3% FBS and used for experiments at 20 days *in vitro*. Cells were routinely serum starved for 24h (and therefore deprived of serum HA) before adding HA.

Antibodies and Reagents: Monoclonal rat anti-CD44 antibody (Clone: 020; Isotype: IgG_{2b}; obtained from CMB-TECH, Inc., San Francisco, CA.) interacts with a common determinant of

the CD44 class of glycoproteins including CD44s (the standard form), and CD44 variant isoforms. This anti-CD44 antibody also recognizes a determinant of the HA-binding region common to CD44 and its principal variant isoforms (Bourguignon, et al, 2000; Bourguignon, et al, 2001a; Bourguignon, et al, 2001b; Bourguignon, et al, 2004). This rat anti-CD44 was routinely used for HA-related blocking experiments and immunoprecipitation. Rabbit anti-phospho-threonine antibody and rabbit anti-phospho-serine antibody were obtained from Zymed Laboratories Inc. Rabbit anti-PKNγ and mouse anti-Rac1 were obtained from Santa Cruz Biotechnology. Mouse anti-His and mouse anti-cortactin antibody (clone 4F11) were purchased from Invitrogene and Upstate Biotechnology (Lake Placid, NY), respectively. GST-tagged Rac1 was obtained from Calbiochem. Cytochalasin D was purchased from Sigma. High molecular weight HA polymers (~10^6 daltons) (Healon^{TM}) were purchased from Amersham Pharmacia Biotech.

Method for Preparing His-tagged Dominant-Negative Form [containing ACC domains] of PKNγ Kinase: The cDNA fragment encoding the ACC domains of PKNγ (aa98-aa256) was generated by reverse transcription-polymerase chain reaction (RT/PCR) using two specific primers (5'-GGTGCAGCAGAAATTGGATGA-3' and 5'-CTTTGACGTGGACTTAGTGTTGGTG-3'). PCR product digested with EcoR I and Hind III was purified with QIAquick PCR purification Kit (Qiagen). The PKNγ-ACC fragment cDNA was subsequently cloned into pcDNA3.1/HisC vector that contains Xpress-epitope to create His-tagged PKNγ-ACCcDNA. The inserted ACC domain sequence was confirmed by nucleotide sequencing analyses. This His-tagged PKNγ-ACC cDNA was then used for transient expression in astrocytes as described below.

Cell Transfection: To establish a transient expression system, cultured astrocytes were transfected with various plasmid DNAs (e.g. His-tagged PKNγ-ACC domain cDNA or vector alone) using lipofectamin 2000 methods (Invitrogen, Carsbad, CA). Briefly, cells were plated at a density of 2 x 10^6 cells per 100 mm dish and transfected with 25μg plasmid cDNA/dish using

lipofectamin 2000. Transfected cells were grown in the culture medium for at least 24-48 h. Various transfectants were then analyzed for their protein expression and functional properties as described below.

Measurement of Rac1 Activation: Cultured astrocytes (~5.0 x 10^5 cells) were incubated in a buffer containing 118 mM KCl, 5 mM NaCl, 0.4 mM $CaCl_2$, 1 mM EGTA, 1.2 mM Mg-acetate, 1.2 mM KH_2PO_4, 25 mM Tris-HCl (pH 7.4), 20 mg/ml BSA followed by adding [^{35}S]GTPγS (12.5 μCi). Subsequently, cells were electroporated at 25 microfarads and 2.0 kV/cm followed by incubating with 50μg/ml HA [in the presence or absence of rat anti-CD44 antibody (50μg/ml)] or without any HA treatment at 37^{o}C for 10 min. [^{35}S]GTPγS labeled cells were then solubilized by NP-40 followed by incubating with mouse anti-Rac1 IgG (5μg/ml) plus goat anti-mouse conjugated beads. The amount of [^{35}S]GTPγS-Rac1 associated with anti-Rac1-conjugated immuno-beads was measured by a gamma-counter.

Immunoblotting and Immunoprecipitation Techniques: Cultured astrocytes (untransfected cells, PKNγ-ACCcDNA-transfected cells or vector-transfected cells) grown in 0.03mM Ca^{2+} were treated with no HA or with HA (50μg/ml) or pretreated with anti-CD44 antibody followed by adding HA (50μg/ml) at 37^{o}C for various time intervals (5min, 10min, 15min, 30min, 2h, 24h, 36h and 48h). These cells were then solubilized in 50mM HEPES (pH 7.5), 150mM NaCl, 20mM $MgCl_2$, 1.0% Nonidet P-40 (NP-40), 0.2mM Na_3VO_4, 0.2mM phenylmethylsulfonyl fluoride, 10μg/ml leupeptin, and 5μg/ml aprotinin. The sample was then analyzed by SDS-PAGE in a 5% or 7.5% polyacrylamide gel. Separated polypeptides were then transferred onto nitrocellulose filters. After blocking non-specific sites with 2% bovine serum albumin, the nitrocellulose filters were incubated with each of the specific immuno-reagents [e.g. rat anti-CD44 IgG (5μg/ml), or rabbit anti-PKNγ (5μg/ml), or rabbit anti-PLCγ1 (5μg/ml), or mouse anti-cortactin (5μg/ml) or mouse anti-His antibody (5μg/ml)] followed by incubating with horseradish peroxidase (HRP)-labeled goat anti-rat IgG, or HRP-labeled goat anti-rabbit IgG or HRP-labeled goat anti-mouse

IgG. The blots were then developed by the ECL™ system (Amersham Co.). For analyzing the recruitment of endogenous PKNγ into CD44 complex, cells [either treated with HA (50μg/ml) or without any HA treatment] were solubilized by 1.0% NP-40 and immunoprecipitated with rat anti-CD44 antibody followed by anti-PKNγ-mediated immunoblot.

Untransfected astrocytes [untreated or pretreated with cytochalasin D (20μg/ml) for 1h at 37^{o}C] or astrocytes transfected with PKNγ-ACCcDNA (or vector alone) were incubated with HA (50μg/ml) at 37^{o}C for 10 min [or pre-treated with anti-CD44 antibody followed by adding HA (50μg/ml) or incubated with no HA]. These cells were then immunoprecipitated with anti-PLCγ1 (or anti-cortactin) antibody followed by immunoblotting with anti-phospho-serine/anti-phospho-threonine or anti-Rac1/anti-His, respectively. Subsequently, these blots were then developed using ECL chemiluminescence reagent according to the manufacturer's instructions. During these immunological analyses, an equal amount of cellular protein (50μg/ml) immunoprecipitated with the antibody was applied to SDS-PAGE followed by immunoblot analyses.

PKNγ-Mediated Protein Phosphorylation Assay *In Vitro*: The PKNγ kinase reaction was carried out in 50 μl of the reaction mixture containing 40 mM Tris-HCl (pH7.5), 2 mM EDTA, 1 mM DTT, 7 mM $MgCl_2$, 0.1% CHAPS, 0.1μM calyculin A, 100μM ATP, 100ng PKNγ [isolated from astrocytes (untransfected or transfected with His-tagged PKNγ-ACCcDNA or vector only) using anti-PKNγ-conjugated Sepharose beads] and 1μg astrocyte cortactin (isolated from astrocytes using anti-cortactin-conjugated Sepharose beads) in the presence of Rac1 (incubated with 200μM GDP or 200μM GTP). After incubation for 30 min at 30^{o}C, the reaction mixtures were immunoprecipitated with anti-cortactin-beads, boiled in SDS-sample buffer and subjected to SDS-PAGE. The protein bands associated with anti-cortactin-beads were revealed by anti-phospho-serine/anti-phospho-threonine-mediated immunoblot or anti-cortactin-mediated immunoblot, respectively. In some cases, PKNγ [isolated from astrocytes (untransfected or transfected with His-tagged PKNγ-ACCcDNA or vector treated with HA or no HA) using anti-

PKNγ-conjugated Sepharose beads] was incubated with the reaction mixture containing 40mM Tris-HCl (pH 7.5), 2mM EDTA, 1mM DTT, 7mM $MgCl_2$, 0.1% CHAPS, 0.1μM calyculin A, 10μCi of [γ-^{32}P]ATP (5000Ci/mmol), and 1μg astrocyte cortactin (isolated from astrocytes using anti-cortactin-conjugated Sepharose beads). After 30min at 30^{o}C, reactions were then terminated by adding 20% cold trichloroacetic acid (TCA); and 2mg/ml BSA was then added as a carrier. TCA precipitated proteins were spotted on 3MM filter papers followed by extensive wash with 10% TCA. The radioactivity associated with TCA-precipitated materials was analyzed by liquid scintillation counting.

***In vitro* Scratch Wound Model:** A scratch wound was made by scraping the cell monolayer (untransfected, transfected with PKNγ-ACCcDNA or vector alone) across the cover glass with a sterile cell lifter according to procedures described previously (Yu et al., 1993; Mukhin et al., 1998). We changed the culture medium immediately after wounding to prevent the medium from being conditioned with cell debris and factors released from deteched cells. Wounded cultured were incubated with 50μg/ml HA (or no HA or with anti-CD44 antibody pretreatment followed by HA addition) for various time intervals (e.g. 0, 4h, 12h or 24h) at 37^{o}C. At different time intervals after wounding, astrocytes were then fixed with 4% paraformaldehyde in 0.1M phosphphate-buffered saline (PBS, pH 7.4) at room temperature for 1h. Both morphological changes and cell migration were analyzed by an inverted phase-contrast microscope.

Double immunofluorescence staining of astrocytes using *in vitro* scratch wound models: To test the effects of HA on cultured astrocytes (untransfected, transfected with PKNγ-ACCcDNA or vector alone) under *in vitro* wounding conditions, a scratch wound were made by scraping the cell monolayer across the cover glass with sterile cell lifter as described above. After wounding, the culture medium was incubated with HA (50μg/ml) (in the presence or absence of anti-CD44) or incubated with no HA for various time intervals (0, 18h or 24h). Subsequently, astrocytes were fixed with 2% paraformaldehyde and stained with fluorescein (FITC)-labeled rat anti-CD44 IgG. These FITC-labeled cells were then rendered permeable by ethanol treatment followed by

incubating with Texas Red-conjugated anti-Rac1 IgG or pholloidin. To detect non-specific antibody binding, FITC-conjugated anti-CD44 or Texas Red-conjugated Rac1 IgG or pholloidin labeled cells were incubated with FITC-conjugated normal rat IgG or Texas Red-conjugated normal rabbit/normal mouse, respectively. No labeling was observed in such control samples. These fluorescein- and Texas red-labeled samples were examined with a confocal laser scanning microscope.

F-Actin Cross-Linking Assay: The procedures for conducting F-actin cross-linking experiments were the same as those described previously (Huang et al., 1997; Huang et al., 1998; Bourguignon et al., 2004) with some modifications. Unphosphorylated cortactin or PKNγ phosphorylated cortactin (as described above)(50-100nM) in 50µl of TKM buffer [50mM Tris-HCl (pH7.4), 134mM KCl and 1mM $MgCl_2$] was mixed with an equal volume of 8µM of ^{125}I-labeled F-actin followed by a 30 min incubation at room temperature. Subsequently, the mixture was centrifuged at 25,000 x g for 10 min at room temperature. The supernatant was then collected and the radioactivity in this fraction was counted. The decrease (or loss) of radioactivity in the supernatant fraction reflects F-actin precipitation due to the cross-linking reaction (Bourguignon et al., 2004). The F-actin cross-linking reaction in the presence of unphosphorylated cortactin (control) is designated as 100%. In some cases, both phosphorylated cortactin (from vector-transfected cells treated with HA) or unphosphorylated cortactin (isolated from vector-transfected cells treated with no HA or from PKNγ-ADDcDNA-transfected cells treated with no HA or with HA) were isolated using anti-cortactin-conjugated Sepharose beads. These cortactin samples were then used for the F-actin cross-linking reaction as described above. Unphosphorylated cortactin isolated from vector-transfected cells treated with no HA (control) was designated as 100%.

Transwell cell migration assays: Twenty-four transwell units were used for monitoring *in vitro* cell migration as described previously (Bourguignon et al., 2000; 2001a; 2001b). Specifically, the 5 µm porosity polycarbonate filters (CoStar Corp., Cambridge, MA) were used for the cell migration assay. Cultured astrocytes (untransfected, transfected with PKNγ-ACCcDNA or vector alone) [in

the presence or absence of rat anti-CD44 antibody (5μg/ml) or 20μg/ml cytochalasin D] (1 x 10^4 cells/well) were placed in the upper chamber of the transwell unit. The medium containing 50μg/ml HA or no HA was placed in the lower chamber of the transwell unit. After 18h incubation at 37°C in a humidified 95% air/5% CO_2 atmosphere, vital stain MTT [3-(4,5-dimethyl thiazol-2-yl)-2,5-diphenyl tetrazolium bromide] (Sigma Co.) was added at a final concentration of 0.2mg/ml to both the upper and the lower chambers and incubated for additional 4h at 37°C. The CD44-specific cell migration was determined by subtracting non-specific cell migration (i.e. cell migrate to the lower chamber in the presence of anti-CD44 antibody treatment). Cell migration in untreated cultured astrocytes (control) or in astrocytes treated with no HA (or vector-transfected cells treated with no HA) is designated as 100%.

RESULTS

HA-CD44 Interaction in Cultured Astrocytes: CD44 is one of the major hyaluronan (HA) cell surface receptors (Underhill 1992) in many different cell types, including astrocytes (Haegel et al., 1993). Immunoblotting with monoclonal rat anti-CD44 antibody showed that a single band of CD44 protein (molecular mass ~85kDa) was detected in cultured astrocytes isolated from mouse brain (Fig. 1, lane 2). We conclude that the expression of CD44 in cultured astrocytes, as shown by anti-CD44-mediated immunoblot, is specific since no protein was detected in these cells using normal rat IgG (Fig. 1, lane 1). By employing a "scratch wound" assay with cultured astrocytes, we found that HA induced CD44-associated membrane projections (Figs. 2A-c and 2A-d) and CD44-F-actin colocalization in membrane protrusions at the wounding edges (Fig. 2B-d, e, f). In contrast, very few CD44-F-actin-associated membrane projections were detected in astrocytes not treated with HA (Figs. 2A-a, b and 2B-a, b, c). Following the formation of a scratch wound, astrocytes were noted to polarize perpendicularly to the scratch and then migrate to close the wound in the presence of HA (Figs. 3A-c, 3A-d and 3B-b). In contrast, pretreatment of cultured astrocytes with anti-CD44 antibody followed by HA addition (Figs. 3A-e, 3A-f and 3B-c) or

without any HA treatment (Fig. 3A-a, 3A-b and 3B-a) resulted in a great reduction in migration and wound closure. Using a Transwell cell migration assay, we also observed that a higher level of cell migration occurred with HA-treated astrocytes as compared to untreated cells (Table 1). Cultured astrocytes pretreated with anti-CD44 antibody or cytochalasin D (an inhibitor known to impair filamentous actin function), showed significantly less HA-mediated migration (Table 1). These findings clearly indicate that HA promotes actin cytoskeleton-mediated astrocyte migration in a CD44-dependent manner.

HA-Stimulated Rac1 Signaling and CD44-PKNγ Kinase Association in Cultured Astrocytes: The binding of HA to CD44 is known to induce important changes in certain RhoGTPases such as Rac1 (Bourguignon et al., 2000; 2001a). Using an *in vitro* [^{35}S]GTPγS binding assay, we determined that Rac1 isolated from mouse cultured astrocytes displayed specific guanine nucleotide binding activity (Table 2). In particular, we demonstrated that the addition of HA to CD44-expressing astrocytes caused almost a three-fold increase in the binding of [^{35}S]GTPγS to Rac1 as compared to the amount of binding present in untreated astrocytes (Table 2), or in astrocytes pretreated with anti-CD44 antibody followed by HA treatment (Table 2). Double immunofluorescence staining data indicated that HA also promoted Rac1 association with CD44 in the membrane projections of astrocytes at the wounding edges (Fig. 2B-g, h, i). These findings suggest that HA and CD44 are directly involved in the activation of Rac1 in cultured astrocytes.

Several lines of evidence indicate that PKNγ binds to RhoGTPases (e.g. Rac1), and that PKNγ's activity is upregulated in the presence of the GTP-bound form of Rac1 (Quilliam et al., 1996; Vincent and Settleman, 1997). In order to identify possible downstream targets for the activated Rac1 in astrocytes, we focused our investigation on PKNγ kinase (also called PRK2 kinase). First, using a specific anti-PKNγ immunoblot technique, we determined that PKNγ (molecular mass ~120kD) was expressed in astrocytes (data not shown). Next, we addressed the question of whether there is an interaction between CD44 and PKNγ in cultured astrocytes. To

this end we carried out anti-CD44-mediated immunoprecipitation followed by anti-PKNγ immunoblot (Fig. 4A-a) or anti-CD44 immunoblot (Fig. 4A-b), respectively, using untreated astrocytes. Our results showed that a low level of PKNγ (Fig. 4A-a, lane 1) was present in the anti-CD44-immunoprecipitated materials (Fig. 4A-b, lane 1). Subsequently, we determined that HA treatment induced the recruitment of a significant amount of PKNγ (Fig. 4A-a, lane 2) into the CD44-PKNγ complex (Fig. 4A-b, lane 2). These findings clearly establish that CD44 and PKNγ are closely associated with each other, particularly following HA treatment of cultured astrocytes.

Cortactin Serves as a Cellular Substrate for Rac1-Dependent PKNγ Kinase and Interacts with Filamentous Actin (F-Actin): Although GTPase-activated PKNγ has been shown to regulate actin cytoskeleton organization (Bourguignon et al., 2004), the specific cytoskeletal components regulated by PKNγ in HA-mediated CD44 signaling in astrocytes have not been clearly defined. In this study we observed that PKNγ kinase isolated from astrocytes was capable of phosphorylating cortactin at both serine (Fig. 4B-a) and threonine residues (Fig. 4B-b) [as detected by anti-phospho-serine and anti-phospho-threonine-mediated immunoblot, respectively followed by reblotting with anti-cortactin antibody (Fig. 4B-c)] in the presence of activated Rac1 (GTP-bound Rac1) (Figs. 4B-a, lane 3 and 4B-b, lane 3) [and to a much lesser extent with GDP-Rac1 treatment (Figs. 4B-a, lane 2 and 4B-b, lane 2)]. The level of serine/threonine phosphorylation of cortactin was relatively low when PKNγ was not incubated with any Rac1 (Figs. 4B-a, lane 1 and 4B-b, lane 1). These results suggest that cortactin phosphorylation by PKNγ involves Rac1 in a GTP-dependent fashion.

Further analyses indicated that the level of serine and threonine phosphorylation of cortactin in cultured astrocytes [as detected by anti-cortactin-mediated immunoprecipitation followed by immunoblotting with anti-serine (Fig. 4C-a) or anti-threonine (Fig. 4C-b) or anti-cortactin (Fig. 4C-c), respectively] was significantly enhanced in astrocytes treated with HA (Fig. 4C-a, lane 2; Fig. 4C-b, lane 2). In contrast, cortactin serine and threonine phosphorylation was

relatively low in astrocytes without any HA treatment (Fig. 4C-a, lane 1; Fig. 4C-b, lane 1). These observations strongly support the conclusion that cortactin phosphorylation is induced by HA.

It is well known that cortactin is an important actin binding protein (Huang et al., 1997; Huang et al., 1998). Our data indicated that cortactin with a low level of phosphorylation (in the absence of PKNγ) (Fig. 4B-lane 1) or in the presence of PKNγ and unactivated Rac1 (GDP-bound Rac1) (Fig. 4B-lane 2), was capable of cross-linking the actin filaments into bundles *in vitro* (Table 3). However, serine/threonine phosphorylation of cortactin by Rac1 (GTP-bound form)-activated PKNγ (Fig. 4B-lane 3) significantly decreased its ability to bind to filamentous actin (Table 3). These results are consistent with previous findings suggesting cortactin (phosphorylated vs. unphosphorylated forms) plays a critical role as a filamentous actin (F-actin) modulator required for cytoskeleton reorganization.

Effects of PKNγ-ACC domains on Cortactin Phosphorylation, Actin Binding and Astrocyte Migration: Several studies have determined that the N-terminal antiparallel coiled-coil (ACC) domains of PKNγ (Fig. 5A-a) bind to RhoGTPases (e.g. Rac1) and upregulate PKNγ's activity in the presence of the GTP-bound form of Rac1 (Quilliam et al., 1996; Vincent and Settleman, 1997; Bourguignon et al., 2004). These findings suggest that the PKNγ-ACC domains play an important role in regulating the activation of Rac1-dependent PKNγ kinase. In order to confirm that the PKNγ-ACC domain regulate astrocyte signaling, PKNγ-ACC domain cDNA was cloned into a His tagged expression vector pcDNA 3.1 (Fig. 5A-b) and then introduced into cultured astrocytes by a transient transfection. To test the interaction between the PKNγ-ACC domain and Rac1, we incubated purified His-tagged PKNγ-ACC domains with either GDP- or GTP-loaded forms of Rac1-GST conjugated beads. Bound proteins were detected by immunoblotting with anti-His antibody (Fig. 5B). Our results indicated that PKNγ-ACC domains appeared to preferentially bind to GTP-bound Rac1 (Fig. 5B, lane 2), and to a much lesser extent to GDP-bound Rac1 (Fig. 5B, line 1). These results agree with previous findings that PKNγ-ACC

domains are capable of binding to Rac1 in a GTP-dependent manner.

In order to examine the effects of PKNγ-ACC fragment overexpression on Rac1 interaction with endogenous PKNγ, we transfected cultured astrocytes with His-tagged PKNγ-ACCcDNA (or vector alone). Our data showed that endogenous PKNγ was expressed at comparable levels in vector-transfected (Fig. 5C-b, lane 1 and lane 2) and PKNγ-ACCcDNA-transfected astrocytes (Fig. 5C-b, lane 3 and lane 4). Furthermore, we observed that a low levels of endogenous Rac1 and PKNγ were co-precipitated in untreated vector-transfected astrocytes (Fig. 5C-a, lane 1; Fig. 5C-b, lane 1). Moreover, we demonstrated that HA induced an additional recruitment of endogenous Rac1 (Fig. 5C-a, lane 2) into a complex with PKNγ (Fig. 5C-b, lane 2) in vector-transfected astrocytes. These results suggest that the recruitment of endogenous Rac1 into PKNγ in cultured astrocytes is HA-dependent. In addition, our observations indicated that transfection of cultured astrocytes with PKNγ-ACCcDNA not only caused a significant inhibition of HA-mediated recruitment of endogenous Rac1 (Fig. 5C-a, lane 4) to PKNγ (Fig. 5C-b, lane 4), but also decreased the basal level of endogenous Rac1 (Fig. 5C-a, lane 3) association with PKNγ (Fig. 5C-b, lane 3). These findings establish the fact that the PKNγ fragment containing ACC domains acts as a potent competitive inhibitor of endogenous Rac1 binding to PKNγ during HA-mediated signaling in cultured astrocytes.

In addition, we determined that phosphorylation of cortactin was stimulated using PKNγ isolated from vector-transfected astrocytes treated with HA (Fig. 6A-b). In contrast, very little cortactin phosphorylation was observed using PKNγ isolated from vector-transfected astrocytes treated with no HA (Figs. 6A-a). We also found that cortactin phosphorylation was greatly blocked using PKNγ isolated from PKNγ-ACCcDNA-transfected astrocytes treated with HA (Fig. 6A-d) or without HA (Fig. 6A-c). Further analyses indicated that unphosphorylated cortactin (treated by PKNγ kinase isolated from vector-transfected cells in the absence of HA) promoted F-actin cross-linking activity *in vitro* (Fig. 6B-a). In contrast, PKNγ kinase-

phosphorylated cortactin (treated by PKNγ kinase isolated from vector-transfected cells in the presence of HA) significantly reduced its ability to cross-link F-actin (Fig. 6B-b). Moreover, we found that unphosphorylated cortactin (treated by PKNγ kinase isolated from PKNγ-ACCcDNA-transfected cells with or without HA addition) retained its F-actin cross-linking properties (Fig. 6B-c and Fig. 6B-d). These results agree with a previous finding suggesting that inhibition of Rac1 binding to PKNγ (Fig. 5C, lane 3 and 4) can effectively impair HA-mediated PKNγ activity and cortactin-F-actin-based cytoskeleton function (Bourguignon et al., 2004).

Furthermore, we demonstrated that cortactin phosphorylation (Table 3B) was greatly enhanced in vector-transfected astrocytes treated with HA as compared with those observed in untreated vector-transfected astrocytes (Table 3B). Cortactin phosphorylation (isolated from vector-transfected astrocytes treated with HA) significantly down-regulated its ability to cross-link filamentous actin (Table 3B). In contrast, the reduction of cortactin phosphorylation (isolated from vector-transfected astrocytes with no HA treatment or from PKNγ-ACCcDNA-transfected astrocytes in the presence or absence of HA) was sufficient to promote cross-linking of actin filaments into bundles *in vitro* (Table 3B). These results demonstrate that the ACC fragment of PKNγ acts as a dominant-negative mutant that downregulates HA-induced Rac1-PKNγ activation and cortactin phosphorylation required for cytoskeleton function.

Furthermore, using Transwell cell migration assays, we observed that cell migration of vector-transfected astrocytes were stimulated during HA treatment (Fig. 7A-a, b). However, transfection of cultured astrocytes with PKNγ-ACCcDNA, resulted in a significant inhibition of HA-mediated astrocyte migration (Fig. 7A-c, d). Similarly, using a scratch wound-induced migration assay of vector-transfected astrocytes, we found a faster rate of migration occurring with HA-treated cells following wounding (Fig. 7B-(I)-c, d; 7B-(II)-b). In contrast, very little cell migration was detected in vector-transfected astrocytes that were not treated with HA (Fig. 7B-(I)-a, b; 7B-(II)-a). We also noted that overexpression of PKNγ-ACC in astrocytes transfected with PKNγ-ACCcDNA significantly reduced cell migration under wounding conditions either in

the presence (Fig. 7B-(I)-g,h; 7B-(II)-d) or absence of HA (Fig. 7B-(I)-e,f; 7B-(II)-c). Thus, HA-mediated Rac1-PKNγ signaling and cytoskeleton function are directly involved in astrocyte migration following mechanical injury *in vitro*.

DISCUSSION

Astrocytes are the major glial cell type in the central nervous system (CNS), and play an essential role in maintaining the physiological function of neurons (Fitch and Silver, 2001; Barres and Barde, 2000). In the CNS, astrocytes often display drastic morphological changes when they interact with neurons and the actin cytoskeleton is known to play an important role in the regulation of astrocyte shape changes (Baorto et al., 1992; Ramakers and Moolenaar, 1998; Etienne-Manneville and Hall 2002; Holtje et al., 2005). After CNS injury, astrocytes also undergo morphological changes. For example, the retraction of astrocyte processes has been described as one of the major ultrastructural changes following CNS injury (Sperry et al., 1993). As early as one hour after CNS injury, there are alterations in the astrocyte cytoskeleton and increased glial fibrillary acidic protein (GFAP) immunoreactivity (Goshgarian et al., 1989; Hadley, 1997). Astrocytes that participate in these early activation processes also proliferate and/or migrate to form the glial scar tissue that encases the damaged area (Hadley, 1997). This process, known as "reactive astrogliosis", is considered to be an accurate indicator of neuronal damage and a major hindrance to axonal regeneration following CNS injury (Stichel and Muller, 1998; Nieto-Sampedro, 1999). The abnormal astrocyte migration to the injured sites also correlates with the failure of regrowing axons to transverse this site (Rhodes et al., 2003; Silver and Miller, 2004; Shearer and Fawcett, 2001; Sivron and Schwartz, 1995). Presently, very little is known about the signaling mechanisms that control astrocyte cytoskeletal changes and cellular function (e.g. migration) following injury.

Hyaluronan (HA) is a very high molecular weight glycosaminoglycan consisting of repeating disaccharide units of D-glucuronic acid and N-acetylglucosamine (Tammi et al., 2002). HA production is closely associated with embryogenesis, wound healing and tumorigenesis

(Toole, 2001; Toole, 2004), and has been implicated in the regulation of astrocyte functions during CNS repair and glial scar formation (Asher et al., 1991; Bignami et al., 1992; Bignami and Asher, 1992; Eggli et al., 1992; Struve et al., 2005). However, the cellular and molecular mechanisms by which astrocytes respond to HA are not well understood. The predominant receptor for HA on the cell surface is CD44 (Haegel et al., 1993) CD44 is encoded by a single gene which contains 19 exons (Screaton et al., 1992). The most common form, CD44s (CD44 standard form), contains exon 1-5 (N-terminal 150 amino acids), exon 15 and 16 (membrane proximal 85 amino acids), exon 17 (transmembrane domain), and a portion of exon 17 and 19 (cytoplasmic tail, 70 amino acids) (Screaton et al., 1992). Out of the 19 exons, 12 exons can be alternatively spliced (Screaton et al., 1992). In this study we have determined that the CD44 detected in astrocytes isolated from normal brain tissues is a ~85kDa polypeptide which is the standard form of CD44 (CD44s) (Fig. 1). A number of astrocyte-type gliomas have also been shown to strongly express different CD44 variant (CD44v) isoforms in addition to CD44s (Kuppner et al., 1992; Haegel et al., 1993). HA binds to the external domain of all CD44 isoforms (Underhill, 1992). A previous study showed that the extracellular domain of CD44 can be released from the cell membrane and becomes associated with ECM (e.g. in glia limitants) (Jones, et al, 1997). This finding suggests that CD44's external part is capable of acting in a dominant-negative fashion by blocking the migration-inducing activity of ECM components such as HA. The binding of HA to CD44 also promotes the interaction of CD44's cytoplasmic domain with a variety of signaling proteins and the cytoskeleton (Bourguignon et al., 1998; Bourguignon, 2001; Turley el al., 2002). In particular, HA mediates CD44 association with c-Src kinase which promotes tyrosine phosphorylation of cortactin [a filamentous actin (F-actin)-associated protein] and cytoskeleton function resulting in specific structural changes in the plasma membrane and cell migration (Bourguignon et al., 2001b). These findings strongly suggest that the CD44 provides a direct linkage between the ECM (e.g. HA) and the signaling molecule-regulated cytoskeleton.

It is well documented that both the structural and functional regulation of the actin cytoskeleton is under the control of RhoGTPases [small molecular weight GTPases, (e.g. RhoA, Rac1 and Cdc42)] which act as molecular switches that alternate between the GTP- and GDP-bound states. The "activated" GTP-bound enzymes preferentially interact with downstream effector molecules and modulate their effectors' activities (Hall 1998). HA has been shown to promote the interaction between CD44 and several Rac1-specific guanine nucleotide exchange factors [e.g. Tiam1 (Bourguignon et al., 2000) and Vav2 (Bourguignon et al., 2001a)] thereby up-regulating Rac1 signaling and cytoskeleton-mediated cell functions. Our results clearly indicate that HA promotes Rac1 signaling in astrocytes (Table 2), and that Rac1 together with F-actin co-localize with CD44 in the membrane projections of astrocytes (Fig. 2B). These observations are consistent with previous reports showing activation of Rac1 signaling is involved in cytoskeleton-associated lamellipodia formation in many cell types (Hall 1998). Furthermore, we have utilized an *in vitro* scratch wound assay to analyze astrocyte reactions to injury. Our results indicate that HA stimulates both cell migration and wound closure in a CD44-dependent manner (Fig. 3). These findings suggest that HA-mediated CD44 interaction with Rac1 and the cytoskeleton plays a pivotal role in cytoskeleton function and migration in astrocytes.

In order to identify the possible downstream targets for Rac1 signaling, we have focused on protein kinase N-γ (PKNγ) (also called PRK2) which belongs to a family of serine/threonine kinases and shares high sequence homology with members of the PKC family of enzymes (Mukai, 2003). There are at least three different isoforms of PKN (PKNα PAK-1/PRK-1, PKNβ and PKNγ/PRK2) which have been detected in mammalian cells (Mukai, 2003). PKNγ is known to interact with Rac1 in a GTP-dependent manner and shares a great deal of homology with PKC in the C-terminal region (Quilliam et al., 1996; Vincent and Settleman, 1997; Mukai, 2003). PKNγ also has a unique regulatory region containing antiparallel coiled-coil (ACC) domains which binds to Rac1 directly (Quilliam et al., 1996; Vincent and Settleman, 1997). A previous

study showed that Rac1-activated PKNγ is required for the organization of the cortical cytoskeleton (Bourguignon et al., 2004). In particular, the cytoskeletal protein, cortactin is a prominent substrate for PKNγ kinase (Bourguignon et al., 2004). HA has also been shown to stimulate Rac1-mediated PKNγ phosphorylation of cortactin leading to cytoskeleton function (Bourguignon et al., 2004). In this study we have determined that cortactin is a cellular substrate for PKNγ kinase in astrocytes activated by HA binding to CD44 (Figs. 4 and 6). Two structural features of cortactin, a repeat domain and a carboxyl-terminal SH3 domain, resemble these of neufectin, an F-actin-associated protein and cortactin is considered to be an actin binding protein (Huang et al., 1997; Huang, et al., 1998). Our results indicate that PKNγ [by binding to activated Rac1 (Rac1-GTP form)] is capable of inducing serine/threonine phosphorylation of cortactin (isolated from astrocytes) (Fig. 4). The ability of PKNγ to phosphorylate cortactin in the presence of unactivated Rac1 (Rac1-GDP form) appears to be extremely limited (Fig. 4). These results clearly indicate that PKN acts as one of the downstream effectors of Rac1 signaling, and utilizes cortactin as one of its cellular targets. Both Rac1 signaling (Table 2) and PKNγ-mediated cortactin phosphorylation (Fig. 4) are stimulated by HA. Thus, it appears that Rac1 activated PKNγ-mediated phosphorylation of cortactin is closely coupled with HA-mediated activation in astrocytes. The fact that cortactin phosphorylation by HA-activated Rac1-PKNγ kinase modifies its binding to F-actin suggests that Rac1-mediated PKNγ activity is closely involved in actin cytoskeleton reorganization during astrocyte signaling.

The ACC domain of PKNγ has been found to be involved in the regulation of GTP-dependent PKN function (Quilliam et al., 1996; Vincent and Settleman, 1997; Bourguignon et al., 2004). As shown in Fig. 5, we have determined that the ACC domain is closely associated with Rac1 in a relatively stable complex. Overexpression of the ACC domain by transfection of astrocytes with PKNγ-ACCcDNA (Fig. 5) effectively competes for the binding of endogenous activated Rac1 to PKNγ (Fig. 5), inhibits the ability of PKNγ to phosphorylate cortactin (Fig. 6),

and blocks HA/CD44-mediated cortactin phosphorylation (Fig. 6). In addition, we have confirmed that cortactin phosphorylation by the PKNγ kinase (isolated from untransfected or vector-transfected astrocytes in the presence of HA) significantly decreases its ability to cross-link filamentous actin (Fig. 6). In contrast, the reduction of cortactin phosphorylation (isolated from astrocytes transfected with PKNγ-ACCcDNA with or without HA treatment) allows the cross-linking of actin filaments into bundles (Fig. 6). These results are consistent with previous findings suggesting cortactin plays an important role as a regulator of F-actin-based cytoskeleton function.

Although a number of factors have been shown to be involved in stimulating astrocyte migration, it was not known whether HA/CD44-mediated Rac1-PKNγ signaling participates in the wound closure processes such as migration. In this study we have found that HA promotes astrocyte migration and wound closure in vector-transfected astrocytes following scratch wounding processes (Fig. 7). In contrast, overexpression of the dominant-negative form of PKNγ (PKNγ-ACC fragment) by transfecting astrocytes with PKNγ-ACCcDNA effectively inhibits HA-mediated migration and wound closure in injured astrocytes (Fig, 7). These data strongly suggest that CD44-mediated PKNγ activation is required for HA-dependent migration and *in vitro* wound closure by astrocytes. Taking these results together, we would like to propose the following signaling model: HA-CD44 interaction (step 1) with Rac1-dependent PKNγ kinase activation (step 2) promotes phosphorylation of cortactin (step 3) and cortactin-mediated cytoskeleton function (step 4) leading to astrocyte migration (step 5) (Fig. 8). We believe that the successful identification of these HA/CD44-mediated signaling pathways will provide valuable new insights toward a better understanding of astrocytes migration and may contribute significantly to the improvement of neural tissue regeneration following injury.

Both hyaluronidases (Stern and Jedrzejas, 2006) and reactive oxygen species (ROS) (Soltes et al., 2006) have been implicated in the partial degradation or modifications of HA polymers. Generally, low molecular weight HA-CD44 interaction induces inflammatory or

proliferative genes; whereas high molecular weight HA-CD44 binding promotes migration and transcriptional activation (Nobel, 2002; Lokeshwar et al., 1996; Turley et al., 2002). The question of whether selective activation of CD44 signaling (via high or low-molecular weight HA) induces a pathway-specific effect on astrocyte functions (cytoskeletal reorganization/activation, proliferation, gene expression and migration) and/or glial scar formation following CNS injury is currently under investigation in our laboratory.

ACKNOWLEDGMENT: We gratefully acknowledge Dr. Gerard J. Bourguignon's assistance in the preparation of this paper. We are also grateful for Ms. Christine Camacho's help in organizing graphs/illustrations and Ms. Elizabeth Gum's assistance in cultured astrocyte preparation. This work was supported by United States Public Health grants (R01 CA66163, R01 CA 78633 and P01 AR39448), a VA Merit Review grant and a DOD grant. L.Y.W.B is a VA Research Career Scientist.

REFERENCES

Asher R., Perides G., Vanderhaeghen J.J. and Bignami A. (1991) Extracellular matrix of central nervous system white mateer: demonstration of an hyaluronate-protein complex. *J. Neurosci Res.* **28,** 410-421.

Barres B.A. and Barde Y. (2000) Neuronal and glial cell biology. *Curr. Opin. Neurobiol.* **10,** 642-648.

Baorto D.M., Mellado W. and Shelanski M.L. (1992) Astrocyte process growth induction by actin breakdown. *J. Cell Biol.* **117,** 357-367.

Bignami, A. and Asher R. (1992) some observations on the localization of hyaluronic acid in adult, newborn and embryonal rat brain. *Int J. Dev. Neurosci* **10,** 45-57.

Bignami, A. Asher R. and Perides G. (1992) The extracellular matrix of rat spinal cord: a comparative study on the localization of hyaluronic acid, glial hyaluronate-binding protein and chondroitin sulfate proteoglycan. *Exp Neurol* **17,** 90-93.

Bourguignon L.Y.W., Zhu D. and Zhu H. (1998) CD44 isoform-cytoskeleton interaction in oncogenic signaling and tumor progression. *Front Biosci.* **3,** 637-649.

Bourguignon, L.Y.W. (2001) CD44-mediated oncogenic signaling and cytoskeleton activation during mammary tumor progression. J Mammary Gland Biol. and *Neoplasia* **6,** 287-297.

Bourguignon L.Y.W., Zhu H., Shao L. and Chen Y.W. (2000) CD44 interaction with Tiam1 promotes Rac1 signaling and hyaluronic acid (HA)-mediated breast tumor cell migration. *J. Biol. Chem.* **275,** 1829-1838.

Bourguignon L.Y.W., Zhu H., Zhou B., Diedrich F., Singleton P.A. and Hung M.C. (2001a) Hyaluronan (HA) promotes CD44v3-Vav2 interaction with Grb2-p185^{HER2} and induces Rac1 & Ras signaling during ovarian tumor cell migration and growth. J. *Biol. Chem*. **276,** 48679-48692.

Bourguignon, L.Y.W., Zhu H., Shao L. and Chen Y.W. (2001b) CD44 interaction with c-

Src kinase promotes cortactin-mediated cytoskeleton function and hyaluronic acid (HA)-dependent ovarian tumor cell migration. *J. Biol. Chem.* **276,** 7327-7336.

Bourguignon L.Y.W., Singleton P.A. and Diedrich F. (2004) Hyaluronan/CD44 interaction with Rac1-dependent PKNγ kinase promotes PLCγ1 activation, Ca^{2+} signaling and cortactin-cytoskeleton function leading to keratinocyte adhesion and differentiation. *J. Biol. Chem.* **279,** 29654-29669.

Burbelo P.D., Drechsel D. And Hall A. (1995) A conserved binding motif defines numerous candidate target proteins for both Cdc42 and RacGTPases. *J. Biol. Chem.* **270,** 29071-29074.

Chen Y. and Swanson R.A. (2003) Astrocytes and brain injury. *J. Cereb Blood Flow Metab* **23,** 137-149.

David S. and Lacroix S. (2003) Molecular approaches to spinal cord repair. *Annu Rev. Neurosci.* **26,** 411-440.

Eddleston M. and Mucke L. (1993) Molecular profile of reactive astrocytes-implications for their role in neurologic disease. *Neurosci.* **54,** 15-36.

Eggli P.S., Lucocq J., Ott P., Graber W., van der Zypen E. (1992) Ultrastructural localization of hyaluronan in myelin sheaths of the rat central and rat and human peripheral nervous systems using haylurona-binding protein-gold and link protein-gold. *Neurosci.* **48,**737-744.

Erschbamer M.K., Hofstetter C.P. and Olson L. RhoA, RhoB, RhoC, Rac1, Cdc42, and Tc10 (2005) mRNA levels in spinal cord, sensory ganglia, and corticospinal tract neurons and long-lasting specific changes following spinal cord injury. *J. Comparative Neurol.* **484,** 224-233.

Etienne-Manneville S. and Hall A. (2002) RhoGTPases in cell biology. *Nature* **420,** 629-635.

Fitch M.T. and Silver J. (2001) Astrocytes are dynamic participants in central nervous system development and injury response. In: Glial cell development. (Jessen K.R. and Richardson W.D., ed). New York: Oxford University Press. p.263-277.

Goshgarian, H.G., Yu, X.J. and Rafols, J.A. (1989) Neuronal and glial changes in the rat phrenic nucleus occurring within hours after spinal cord injury. *J. Comp. Neurol.* **284,** 519-530.

Kuppner M.C., van Meir E., Gauthier T., Hamou M.F. and de Tribolet N. (1992) Differential expression of the CD44 molecule in human brain tumors. *Int. J. Cancer* **50,** 575-577.

Hadley, S.D. and Goshgarian, H.G. (1997) Altered immunoreactivity for glial fibrillary acidic protein in astrocytes within 1h after cervical spinal cord injury Exp. Neurol. 146:380-387.

Haydon P.G. (2000) Neuroglial networks: Neurons and glia talk to each other. *Curr. Biol.* **10,** R712-R714.

Haegel H., Tolg C., Hofmann M. and Ceredig R. (1993) Activated astrocytes and T cells express similar CD44 variants. Role of CD44 in astrocyte/T cell binding. *J. Cell Biol.* **122,** 1067-1077.

Hall A. (1998) Rho GTPase and the cytoskeleton. *Science* **279,** 509-514.

Holtje M., Hoffmann A., Hofmann F., Mucke C., Groβe, van Rooijen N., Kettenmann H., Just I. and Ahnert-Hilger G. (2005) Role of RhoGTPase in astrocyte morphology and migratory response during in vitro would healing. *J. Neuro*chem **95,** 1237-1248.

Huang, C., Ni, Y., Wang, T., Gao, Y., Haudenschild, C.C. and Zhan, X. (1997) Down-regulation of the filamentous actin cross-linking activity of cortactin by Src-mediated tyrosine phosphorylation. *J. Biol. Chem.* **272,** 13911-13915.

Huang, C., Liu, J., Haudenschild, C.C. and Zhan, X.J. (1998) The role of tyrosine phosphorylation of cortactin in the locomotion of endothelial cells. *J. Biol.Chem.* **273,** 25770-25776.

Jones L.L., Kreutzberg G.W. and Raivich G. (1997) Regulation of CD44 in the regenerating mouse facial motor nucleus. *Eur J Neurosci.* **9,** 1854-1863.

Jones L.L., Liu Z., Shen J., Werner A., Kreutzberg G.W. and Raivich G. (2000)

Regulation of the cell adhesion molecule CD44 after nerve transaction and direct trauma to the mouse brain. *J. Comp. Neurol.* **426,** 468-492.

Lokeshwar V.B., Iida N, Bourguignon L.Y.W. (1996) The cell adhesion molecule, GP116 is a new CD44 variant (ex14/v10) involved in hyaluronic acid binding and endothelial cell proliferation. *J Biol Chem*.**271,** 23853-23864.

Lee J. Y. and Spicer A.P. (2000) Hyaluronan: a multifunctional, megadalton, stealth molecule. *Curr Opin Cell Biol.* **12,** 581-586.

Mukai H. (2003) The structure and function of PKN, a protein kinase having a catalytic domain homologous to that of PKC. *J. Biochem* **133,** 17-27.

Mukhin, A.G., Ivanova, S.A., Allen, J.W. and Faden, A.I. (1998) Mechanical injury to neuronal/glial cultures in microplates: role of NMDA receptors and pH in secondary neuronal cell death. *J Neurosci Res* **51,** 748-758.

Nieto-Sampedro M. (1999) Neurite outgrowth inhibitors in gliotic tissue. *Adv. Exp. Med. Biol.* **468,** 207-224.

Noble PW. (2002) Hyaluronan and its catabolic products in tissue injury and repair. *Matrix Biology* **25,** 25-29.

Quackenbush E.J., Cruz T.F., Moscarello M.A. and Letarte M. (1985) Identification of three antigens in human brain associated with similar antigens on human leukemic cells. *Biochem J.* **225,** 291-299.

Quilliam L.A., Lambert Q.T., Mickelson-Young L.A., West-wick J.K., Sparks A.B., Kay B.K., Jenkins N.A., Gilbert D.J., Copeland N.G., and Der C.J. (1996) Isolation of a NCK-associated kinase, PRK2, an SH3-binding protein and potential effector of Rho protein signaling. *J. Biol. Chem.* **271,** 28772-28776.

Ramakers G.J.A. and Moolenaar, W.H. (1998) Regulation of astrocyte morphology by RhoA and lysophosphatidic acid. *Exp. Cell Res.* **245,** 252-262.

Rhodes K.E., Moon L.D., and Fawcett J.W. (2003) Inhibiting cell proliferation during formation of the glial scar: effects on axon regeneration in the CNS. *Neurosci.* **120,** 41-56.

Ridet J.L., Malhotra S.K., Privat A. and Cage F.H. (1997) Reactive astrocytes: Cellular and molecular cues to biological function. *Trends Neurosci* **20,** 570-577.

Screaton G.R., Bell M.V., Jackson D.G., Cornelis F.B., Gerth U. and Bell J.I. (1992) Genomic structure of DNA encoding the lymphocyte homing receptor CD44 reveals at least 12 alternatively spliced exons. *Proc. Natl. Acad. Sci . U.S.A.* **89,** 12160-12164.

Stern, R. and Jedrzejas, M.J. (2006) Hyalurinidases: their genomics, structures, and mechanisms of action. *Chem Rev.* **106,**818-839.

Shearer M.C. and Fawcett J.W. (2001) The astrocyte/meningeal cell interface-a barrier to successful nerve regeneration? *Cell Tissue Res.* **305,** 267-273.

Silver J. and Miller J.H. (2004) Regeneration beyond the glial scar. *Nat Rev. Neurosci.* **5,** 146-156.

Sivron T. and Schwartz M. (1995) Glial cell types, lineage and response to injury in rat and fish: Implication for regeneration. *Glia* **13,** 157-165.

Soltes, L., Mendichi, R., Kogan, G., Schiller, J., Stankovska, M., and Arnhold, J. (2006) Degradative action of reactive oxygen species on hyaluronan. *Biomacromolecules* **7,** 659-668.

Song H., Stevens C.F. and Gage F.H. (2002) Astroglia induce neurogenesis from adult neural stem cells. *Nature* **417,** 39-44.

Sperry, M.A. and Goshgarian, H.G. (1993) Ultrastructural changes in the rat phrenuc nucleus developing within 2 h after cervical spinal cord hemisection. *Exp. Neurol.* **120,** 233-244.

Stichel C.C. and Muller H.W. (1998) The CNS lesion scar: new vistas on an old regeneration barrier. *Cell Tissue Res.* **294,** 1-9.

Struve J., Maher P.C., Li Y-Q., Kinney S., Fehlings M.G.,Kuntz, C. IV and Sherman L.S. (2005) Disruption of the hyaluronan-based extracellular matrix in spinal cord promotes astrocyte proliferation. *Glia* **52,** 16-24.

Swanson R.A., Farrell K. and Stein B.A. (1997) Astrocyte energetics, function, and death under conditions of incomplete ischemia: a mechanism of glial death in the penumbra. *Glia* **21,** 142-153.

Tammi M.I., Day A.J. and Turley E.A. (2002) Hyaluronan and homeostasis: a balance act. *J. Biol. Chem.* **277,** 4581-4584.

Tona A. and Bignami A. (1993) Effects of hyaluronidase on brain extracellular matrix in vivo and optic nerve regeneration. *J. Neurosci. Res* **36,** 191-199.

Toole B. P. (2001) Hyaluronan in morphogenesis. *Semin Cell Dev. Biol.* **12,** 79-87.

Toole B.P. (2004) Hyaluronan from extracellular glue to pericellular cue. *Nat Rev Cancer* **4,** 528-539.

Turley E. A., Nobel P.W. and Bourguignon L.Y.W. (2002). Signaling Properties of Hyaluronan Receptors. [Mini-Review] *J. Biol. Chem.* **277,** 4589-4592.

Underhill C. (1992) CD44: the hyaluronan receptor. *J. Cell Sci.* **103,** 293-298.

Ullian E.M., Sapperstein S.K. Christopherson K.S. and Barrer B.A. (2001) Control of synapse number by glia. *Science* **291,** 657-660.

Vincent S. and Settleman, J. (1997) The PRK2 kinase is a potential effector target of both Rho and Rac GTPase and regulates actin cytoskeletal organization. *Mol. Cell Biol.* **17,** 2247-2256.

Yoshinaga C., Mukai H., Toshimori M., Miyamoto M., and Ono Y. (1999) Mutational analysis of the regulatory mechanism of PKN: the regulatory region of PKN contains an arachidonic acid-sensitive autoinhibitory domain. *J. Biochem.* **126,** 475-484.

Yu, A.C.H., Lee, Y-L. and Eng, L.F. (1993) Astroglisis in culture: I. the model and the effect of antisense oligonucleotides on glial fibrillary acidic protein synthesis. *J. Neurosci. Res.* **34,** 295-303.

Table1: Measurement of HA/CD44-dependent and cytoskeleton-mediated astrocyte migration.

A: Effects of Anti-CD44 antibody on HA-dependent and CD44-specific astrocyte migration.

Treatments	**Cell Migration *(% of control)*[a]**
No treatment (control)	**100**
HA treatment	**290±11[b]**
Anti-CD44 IgG pretreatment + HA treatment	**96±3[b]**

B: Effects of cytochalasin D on HA-mediated astrocyte migration.

Treatments	**Cell Migration *(% of control)*[a]**
No drug treatment (control)	**100**
No drug treatment (control) + HA	**288±9[b]**
Cytochalasin D treatment alone	**35±1[b]**
Cytochalsin D treatment + HA	**37±1[b]**

Cultured astrocytes [~1 x 10^4 cells/well in phosphate buffered saline (PBS), pH 7.2] were placed in the upper chamber of the transwell unit. In some cases, cultured astrocytes were pretreated with various agents (e.g. anti-CD44 IgG or cytochalasin D). After 18h incubation at 37^{o}C in a humidified 95% air/5% CO_2 atmosphere, cells on the upper side of the filter were removed by wiping with a cotton swap. Cell migration was determined by measuring the number of cells that migrated to the lower side of the polycarbonate filters containing HA (or no HA) by either MTT staining or standard cell number counting assays. The CD44-specific cell migration was determined by subtracting non-specific cell migration (i.e. cells migrate to the lower chamber in the presence of rat anti-CD44 antibody treatment) from the total migratory cells in the lower chamber. Cells treated with no HA (control) is designated as 100%.

a: Data represent mean ± SEM of cells that migrated to the lower side of the polycarbonate filters and chambers from each sampe.

b: Significantly different ($p<0.001$; ANOVA; n=6) as compared with no treatment (control) sample.

Table 2: Detection of Rac1 activation in cultured astrocytes.

Treatments	**Amount of [^{35}S]GTPγS bound to Rac1 (cpm)** ***(% of control)***[a]
No treatment (control)	**5,500 ± 220 (100%)**
HA treatment	**16,225 ± 575 (295%)**[b]
Anti-CD44 IgG + HA treatment	**5,392 ± 218 (98%)**[b]

Cultured astrocytes (~1.0 x 10^4 cells) were preloaded with [^{35}S]GTPγS (12.5 μCi) using electroporation methods as described in the Materials and Methods. These cells were incubated with 50μg/ml HA at 37^{o}C for 10 min [in the presence or absence of rat anti-CD44 antibody (50μg/ml) or without any HA treatment]. Subsequently, [^{35}S]GTPγS labeled cells were solubilized in 1.0% NP-40 and incubated with mouse anti-Rac1 IgG (5μg/ml) plus goat anti-mouse conjugated beads. The amount of [^{35}S]GTPγS-Rac1 associated with anti-Rac1-conjugated immuno-beads was measured using a gamma counter. Cells treated with no HA (control) is designated as 100%.

a: Data represent mean ± SEM of [^{35}S]GTPγS (cpm) bound to Rac1 in each sample.

b: Significantly different ($p<0.001$; ANOVA; n=5) as compared with no treatment (control) sample.

Table 3: Analyses of cortactin phosphorylation and cortactin-F-actin binding.

A: Measurement of cortactin (phosphorylated by PKNγ) binding to F-actin.

Samples	**Cortactin-Actin Binding (cpm)** ***(% of Control)***[a]
Unphosphorylated Cortactin (using PKNγ alone) (control)	**12,455 ± 622 (100%)**
Phosphorylated Cortactin (using PKNγ + GDP-bound Rac1)	**12,206 ± 366 (98%)**[b]
Phosphorylated Coractin (using PKNγ + GTP-bound Rac1)	**6,975 ± 279 (56%)**[b]

Cortactin isolated from astrocytes was phosphorylated by PKNγ in the presence of GDP-/GTP-bound Rac1 or PKNγ alone. Subsequently, unphosphorylated or Rac1-PKNγ phosphorylated coractin was incubated with ^{125}I-labeled F-actin. The procedures for measuring cortactin-F-actin binding were described in the Materials and Methods. Unphosphorylated cortactin (using PKNγ alone) (control) is designated as 100%.
a: Data represent mean ± SEM of cortactin-actin binding (cpm) in each sample.
b: Significantly different ($p<0.001$; ANOVA; n=5) as compared with unphosphorylated cortactin (using PKNγ alone) (control) sample.

B: Effect of PKNγ-ACCcDNA overexpression on cortactin phosphorylation and cortactin-F-actin binding.

Cells	**Cortactin phosphorylation** ***(% of control)***[a]		**Cortactin-F-actin binding** ***(% of control)***[c]	
	-HA	**+HA**	**-HA**	**+HA**
Vector-transfected cells (control)	100	257±12[b]	100	43±0.4[d]
PKNγ-ACCcDNA-transfected cells	102±4[b]	105±3[b]	101±3.4[d]	103±2.3[d]

The procedures for measuring cortactin phosphorylation and cortactin-F-actin binding using astrocytes transfected with PKNγ-ACCcDNA or vector alone were described in the Materials and Methods.
a: Data represent mean ± SEM of cortactin phosphorylation (cpm) in each sample.
b: Significantly different ($p<0.001$; ANOVA; n=6) as compared with vector-transfected cells with no HA treatment (control) sample.
c: Data represent mean ± SEM of cortactin-^{125}I-F-actin binding (cpm) in each sample.
d: Significantly different ($p<0.001$; ANOVA; n=5) as compared with vector-transfected cells with no HA treatment (control) sample.

FIGURE LEGENDS

Fig. 1: Detection of CD44 expression in cultured astrocytes. Cultured astrocytes were solubilized by 1% Nonidet P-40 (NP-40) buffer followed by anti-CD44-mediated immunoblotting analyses. Immunoblot of astrocytes with normal rat IgG (lane 1), or with rat anti-CD44 antibody (lane 2).

Fig. 2: Morphological analysis and immunofluorescence staining of CD44, F-actin and Rac1 in cultured astrocytes using *in vitro* scratch wound models. A scratch wound was made by scraping the astrocyte monolayer across the cover glass with a sterile cell lifter as described in the Materials and Methods. A-a,b: A phase-contrast photomicrograph (A-a) and anti-CD44-mediated immuno-staining (green in A-b) of cultured astrocytes 4h after wounding in the absence of HA treatment; A-c,d: A phase-contrast photomicrograph (A-c) and anti-CD44-mediated immuno-staining (green in A-d) of cultured astrocytes 4h after wounding in the presence of HA treatment (Note the formation of CD44-associated membrane projections at the wounding edge). [Scale bars for A- (a-d): 10μm]. B-a,b,c: Immuno-colocalization of CD44 (a) and F-actin (b) using FITC-labeled anti-CD44 antibody (green color) (a), Texas Red-labeled phalloidin (red color) (b) and co-localization of FITC-anti-CD44 and Texas Red-phalloidin (c) [an overlay image of (a) and (b)] in cultured astrocytes treated with no HA for 18 hrs following scratch wounding (dotted line represents wounding edge). B-d,e,f: Immuno-colocalization of CD44 (d) and F-actin (e) using FITC-labeled anti-CD44 antibody (green color) (d), Texas Red-labeled phalloidin (red color) (e) and co-localization of FITC-anti-CD44 and Texas Red-phalloidin (f) [an overlay image of (d) and (e)] in cultured astrocytes treated with HA for 18 hrs following scratch wounding (arrows show migratory direction). B-g,h,i: Immuno-colocalization of CD44 (g) and Rac1 (h) using FITC-labeled anti-CD44 antibody (green color) (i), Texas Red-labeled anti-Rac1 (red color) (e) and co-localization of FITC-anti-CD44 and Texas Red-anti-Rac1 (i) [an overlay image of (g) and (h)] in cultured astrocytes treated with HA for 18 hrs following scratch wounding (arrows show migratory direction). [Scale bars for B-(a-i): 50μm].

Fig. 3: Scratch wound-induced migration assays. A scratch wound was made by scraping the astrocyte monolayer across the cover glass with a sterile cell lifter as described in the Materials and Methods. A-a,b: Phase-contrast photomicrographs of cultured astrocytes (treated with no HA) for 0h (a) or 24h (b) after *in vitro* scratch wounding. A-c,d: Phase-contrast photomicrographs of cultured astrocytes (treated with HA) for 0h (c) or 24h (d) after *in vitro* scratch wounding.

A-e,f: Phase-contrast photomicrographs of cultured astrocytes (pretreated with anti-CD44 antibody followed by adding HA) for 0h (a) or 24h (b) after *in vitro* scratch wounding. [Scale bars for A-(a-f): 100μm]. B-Degree of wound closure is expressed as percent of control (24h after scratch wounding in the absence of HA treatment) (a). Astrocytes (treated with HA) for 24h after *in vitro* scratch wounding (b); Astrocytes (pretreated with anti-CD44 antibody followed by adding HA) for 24h after *in vitro* scratch wounding (c). The data are shown as means ±SEM. [**Significantly different (p<0.001; ANOVA; n=5) as compared with untreated (control) sample].

Fig. 4: Characterization of PKNγ in cultured astrocytes.

A: Detection of PKNγ and CD44 in the complex isolated from untreated astrocytes (lane 1) and HA-treated astrocytes (lane 2) by employing anti-CD44-mediated immunoprecipitation followed by immunoblotting with anti-PKNγ (a) or reblotting with anti-CD44 (b) as a loading control. The ratio of PKNγ to CD44 levels was determined by densitometry and the levels were normalized to the untreated astrocyte value (lane 1); The values expressed in Fig. 4A represent an average of triplicate determinations of 5 experiments with a standard deviation less than ±5%

[* Significantly different (p<0.05; Student's t-test) as compared with untreated (control) sample].

B and C: Detection of cortactin phosphorylation by PKNγ *in vitro* (B) and *in vivo* (C).

B: The PKNγ kinase reaction was carried out in the reaction mixture containing ATP, purified PKNγ and cortactin in the presence of Rac1 (incubated with GDP or GTP) as described in the Materials and Methods. Detection of cortactin phosphorylation *in vitro* by incubating cortactin with PKNγ alone (lane 1), or GDP-Rac1-treated PKNγ (lane 2), or GTP-Rac1-treated PKNγ (lane

3) followed by analyzing with anti-phospho-serine (a)/anti-phospho-threonine (b)-mediated immunoblot or anti-cortactin-mediated immunoblot (a loading control) (c). The ratio of phospho-serine/threonine cortactin to total cortactin (the loading control) was determined by densitometry, and the level were normalized to cortactin phosphorylation by PKNγ alone (lane 1); The values expressed in Fig. 4B represent an average of triplicate determinations of 6 experiments with a standard deviation less than ±5%. [* Significantly different ($p<0.05$; ANOVA) as compared with these samples treated with PKNγ alone].

C: Detection of cortactin phosphorylation *in vivo* by employing anti-cortactin-mediated immunoprecipitation followed by immunoblotting with anti-phospho-serine (a) or anti-phospho-threonine (b) or (reblotting with anti-cortactin as a loading control) (c) in cultured astrocytes treated with no HA (lane 1), or with HA (lane 2). [The ratio of phospho-serine/threonine cortactin to total cortactin (the loading control) was determined by densitometry, and the levels were normalized to untreated astrocyte value (lane 1); The values expressed in Fig. 4C represent an average of triplicate determinations of 5 experiments with a standard deviation less than ±5%.

[* Significantly different ($p<0.05$; ANOVA) as compared with untreated (control) samples].

Fig. 5: Interaction between the PKNγ-ACC fragment and Rac1 *in vitro*; and detection of PKNγ-Rac1 complex in PKNγ-ACC cDNA-transfected/vector-transfected cells.

A-Illustration of PKNγ full-length (a) and His-tagged PKNγ-ACCcDNA construct (b).[The ACC1ACC2ACC3 sequence represents the antiparallel coiled-coil fold (ACC domain) and participates in Rac1 binding; C2-like domain functions as an auto-inhibitory domain for PKNγ].

B: Characterization of the binding interaction between His-tagged PKNγ-ACC and GST Rac1-beads *in vitro*. Anti-His-mediated immunoblot of PKNγ-ACC fragment associated with GDP-bound Rac1-beads (lane 1), or with GTP-bound Rac1-beads (lane 2).

C: Analyses of PKNγ-ACC-Rac1 complex formation in astrocyte transfectants: astrocytes (transfected with His-tagged PKNγ-ACCcDNA or vector alone) were solubilized by 1% Nonidet

P-40 (NP-40) buffer. Cell lysates were then used for anti-PKNγ-mediated immunoprecipitation followed by immunoblotting with anti-Rac1 antibody or anti-PKNγ antibody, respectively as described in the Materials and Methods. Anti-Rac1-mediated immunoblot (a) or anti-PKNγ-mediated immunoblot (b) of anti-PKNγ-mediated immunoprecipitated materials isolated from astrocytes transfected with vector alone treated with no HA (lane 1) or with HA (lane 2); or astrocytes transfected with PKNγ-ACCcDNA treated with no HA (lane 3) or with HA (lane 4).

Fig. 6: Detection of PKNγ-mediated cortactin phosphorylation and measurement of the F-actin cross-linking activity of cortactin. A: PKNγ activity was determined by the amount of [γ-^{32}P]ATP incorporation (cpm) into cortactin using PKNγ isolated from astrocytes [transfected with vector alone treated with no HA (a) or with HA (b); or astrocytes transfected with PKNγ-ACCcDNA treated with no HA (c) or with HA (d)]. Unphosphorylated cortactin incubated with PKNγ (isolated from vector-transfected cells in the absence of HA) (control) is designated as 100%. The data are shown as means ±SEM. **Significantly different (p<0.001; ANOVA; n=5) as compared with the control sample. B: Measurement of the F-actin cross-linking activity of cortactin: Purified cortactin treated with PKNγ isolated from astrocytes [transfected with vector alone treated with no HA (a) or with HA (b); or astrocytes transfected with PKNγ-ACCcDNA treated with no HA (c) or with HA (d)] was subjected to F-actin cross-linking analysis as described in the Materials and Methods. The F-actin cross-linking reaction in the presence of unphosphorylated cortactin (using PKNγ isolated from vector-transfected cells treated with no HA) (control) is designated as 100%. The data are shown as means ±SEM. **Significantly different (p<0.001; ANOVA; n=5) as compared with the control sample.

Fig.7: Effects of PKNγ-ACC overexpression on astrocyte migration. **A: Transwell cell migration assays:** Twenty-four transwell units were used for monitoring *in vitro* cell migration as described in the Materials and Methods. Vector-transfected cells treated with no HA) is designated as 100%. (a, vector-transfected cells treated with no HA; vector-transfected cells

treated with HA; PKNγ-ACCcDNA-transfected cells treated with no HA; PKNγ-ACCcDNA-transfected cells treated with HA). The data are shown as means ±SEM. **Significantly different (p<0.001; ANOVA; n=4) as compared with the control sample. **B: Scratch wound-induced migration:** A scratch wound was made by scraping the astrocyte monolayer (treansfected with PKNγ-ACCcDNA or vector alone) across the cover glass with a sterile cell lifter as described in the Materials and methods. B-(I)-a,b: Phase-contrast photomicrographs of vector-transfected astrocytes (treated with no HA) for 0h (a) or 24h (b) after *in vitro* scratch wounding. B-(I)-c,d: Phase-contrast photomicrographs of vector-transfected astrocytes (treated with HA) for 0h (c) or 24h (d) after *in vitro* scratch wounding. B-(I)-e,f: Phase-contrast photomicrographs of PKNγ-ACCcDNA-transfected astrocytes (treated with no HA) for 0h (a) or 24h (b) after *in vitro* scratch wounding. B-(I)-g,h: Phase-contrast photomicrographs of PKNγ-ACCcDNA-transfected astrocytes (treated with HA) for 0h (c) or 24h (d) after *in vitro* scratch wounding. [Scale bars for B-(I)-(c-h): 100μm]. B-(II): Degree of wound closure is expressed as percent of control (24h after scratch wounding of vector-transfected cells in the absence of HA treatment is designated as 100%). Vector-transfected astrocytes (treated with no HA) (a) or treated with HA (b) for 24h after *in vitro* scratch wounding; PKNγ-ACCcDNA-transfected astrocytes (treated with no HA) (c) or treated with HA (d) for 24h after *in vitro* scratch wounding. The data are shown as means ±SEM. [**Significantly different (p<0.001; ANOVA; n=5) as compared with the control sample].

Fig. 8: A proposed model for the interaction between HA/CD44-mediated Rac1-PKNγ activation and cortactin-cytoskeleton binding during astrocyte migration. HA-CD44 interaction (step 1) with Rac1-dependent PKNγ kinase activation (step 2) promotes phosphorylation of cortactin (step 3) and cortactin-mediated cytoskeleton function (step 4) leading to astrocyte migration (step 5).

Figure 1

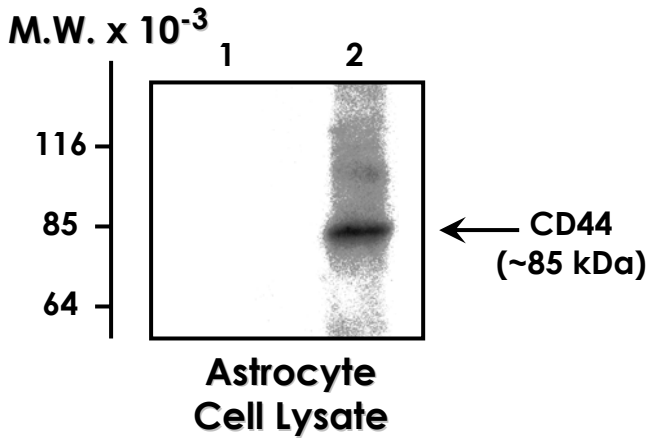

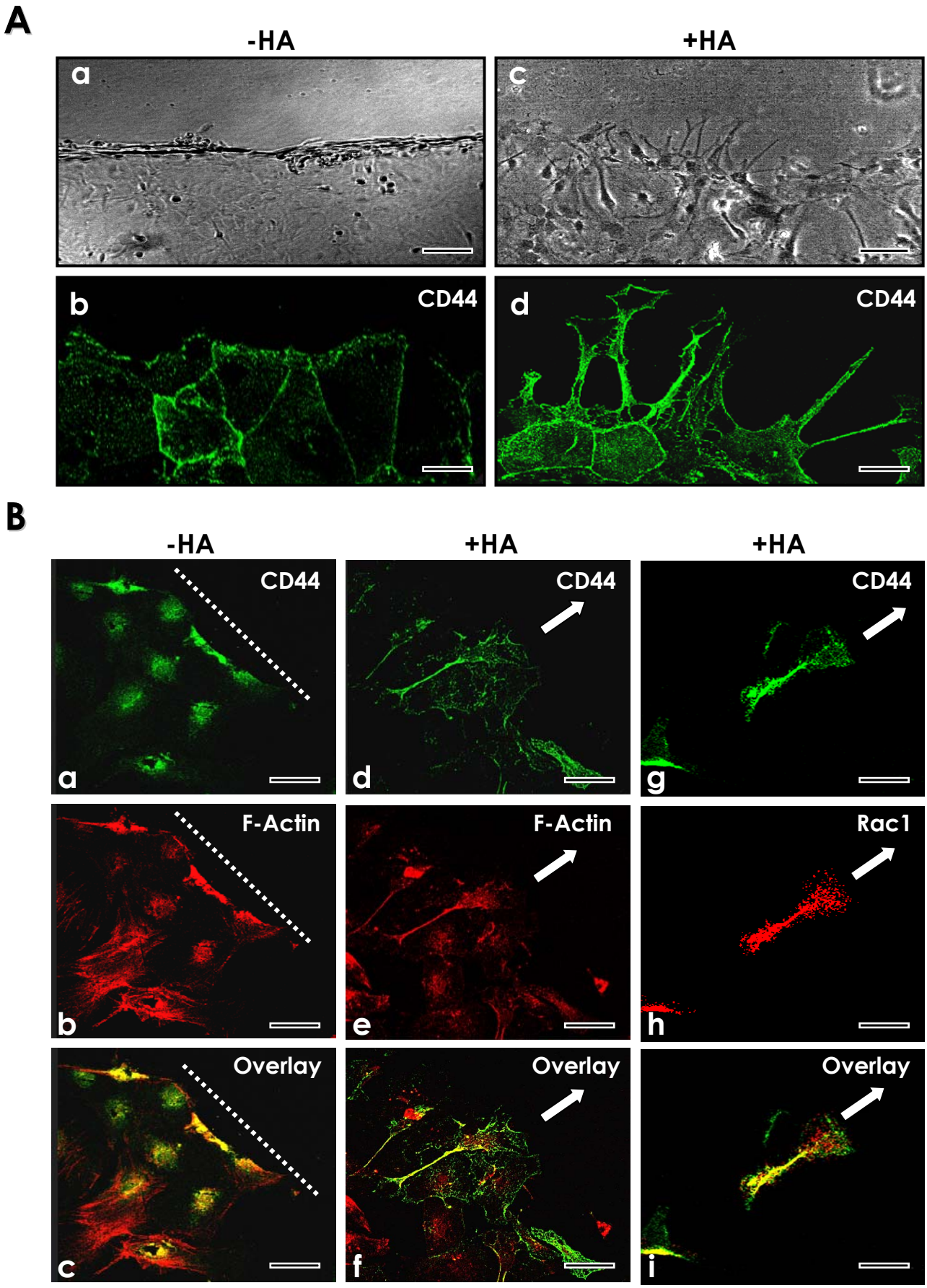
A
-HA
+HA
a
c
b
CD44
d
CD44
B
-HA
+HA
+HA
CD44
CD44
CD44
a
d
g
F-Actin
F-Actin
Rac1
b
e
h
Overlay
Overlay
Overlay
c
f
i

A

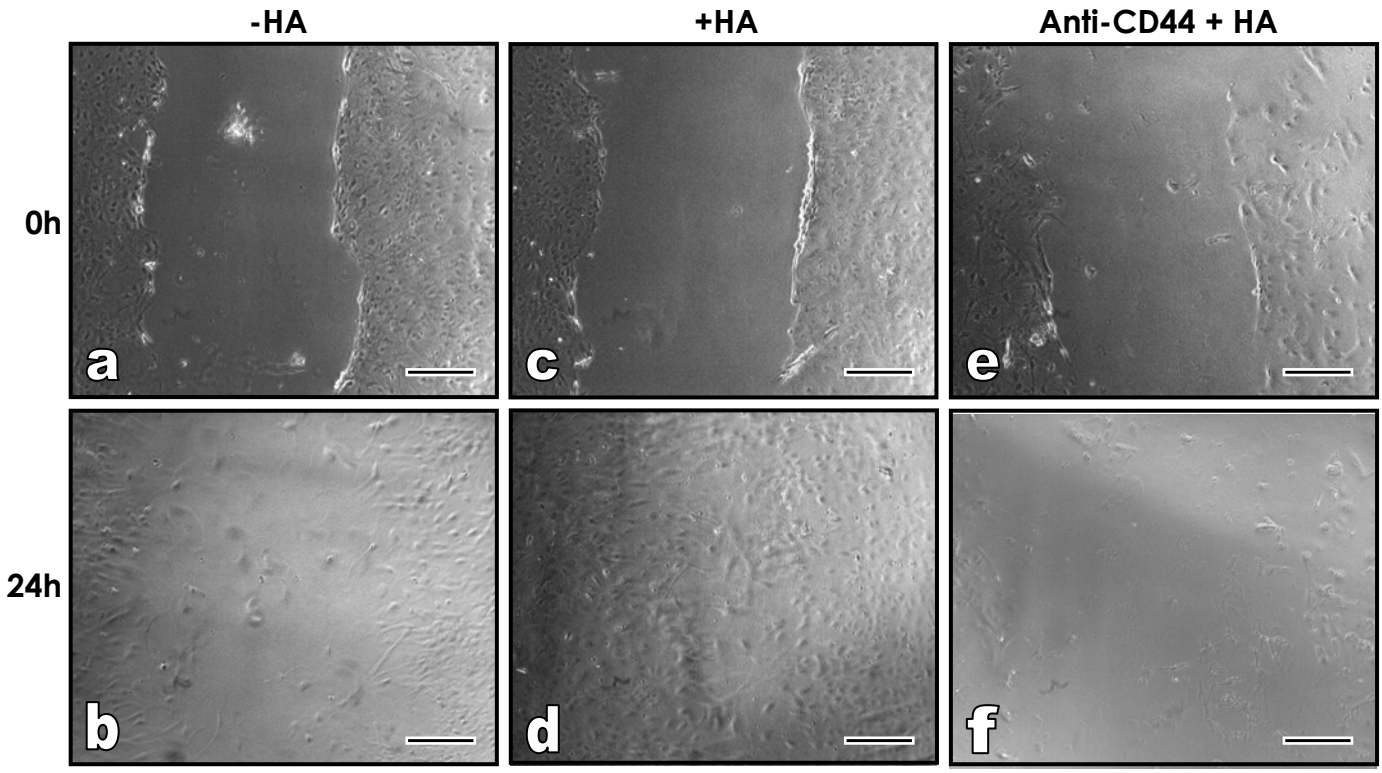
-HA
+HA
Anti-CD44 + HA
0h
24h
a
b
c
d
e
f

B

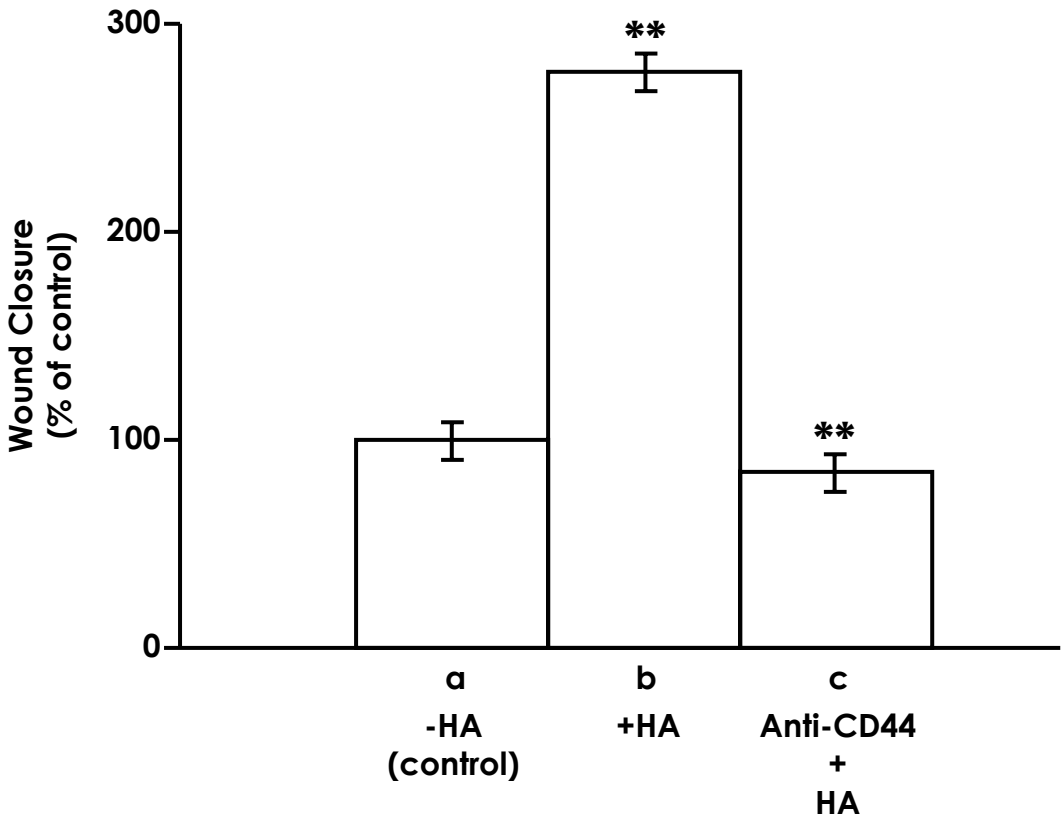
Wound Closure
(% of control)
300
200
100
0
**
**
a
-HA
(control)
b
+HA
c
Anti-CD44
+
HA

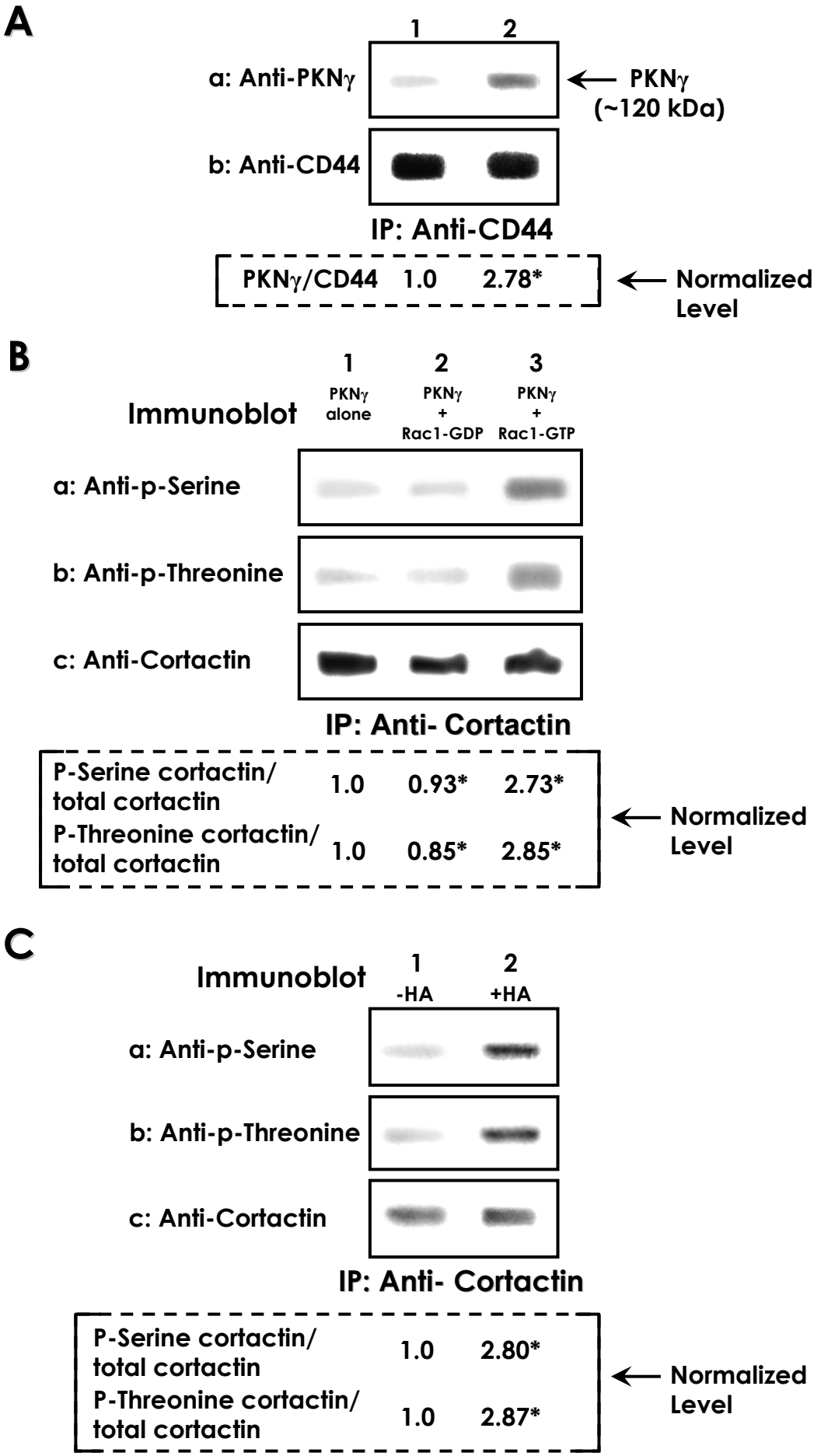
A
1
2
a: Anti-PKNγ
PKNγ
(~120 kDa)
b: Anti-CD44
IP: Anti-CD44
PKNγ/CD44 1.0 2.78*
Normalized Level
B
Immunoblot
1
PKNγ alone
2
PKNγ + Rac1-GDP
3
PKNγ + Rac1-GTP
a: Anti-p-Serine
b: Anti-p-Threonine
c: Anti-Cortactin
IP: Anti- Cortactin
P-Serine cortactin/ total cortactin 1.0 0.93* 2.73*
P-Threonine cortactin/ total cortactin 1.0 0.85* 2.85*
Normalized Level
C
Immunoblot
1
-HA
2
+HA
a: Anti-p-Serine
b: Anti-p-Threonine
c: Anti-Cortactin
IP: Anti- Cortactin
P-Serine cortactin/ total cortactin 1.0 2.80*
P-Threonine cortactin/ total cortactin 1.0 2.87*
Normalized Level

A

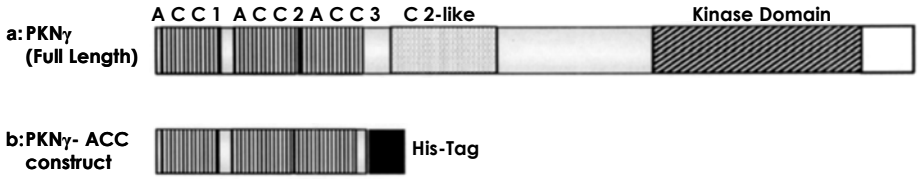
A C C 1 A C C 2 A C C 3
C 2-like
Kinase Domain
a: PKNγ
(Full Length)
b: PKNγ- ACC
construct
His-Tag

B

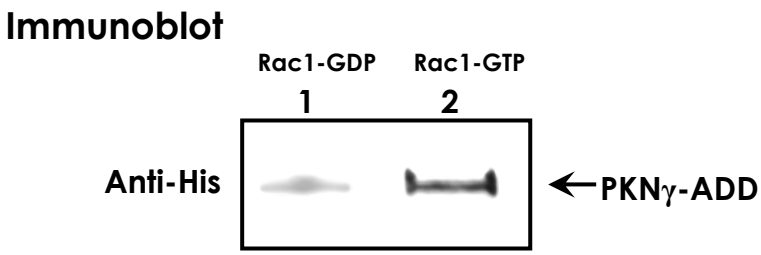
Immunoblot
Rac1-GDP
Rac1-GTP
1
2
Anti-His
PKNγ-ADD

C

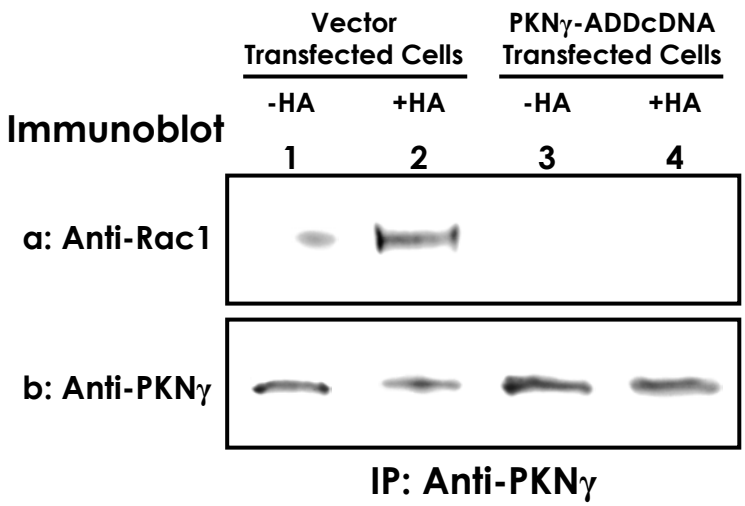
Vector
Transfected Cells
PKNγ-ADDcDNA
Transfected Cells
-HA
+HA
-HA
+HA
Immunoblot
1
2
3
4
a: Anti-Rac1
b: Anti-PKNγ
IP: Anti-PKNγ

A

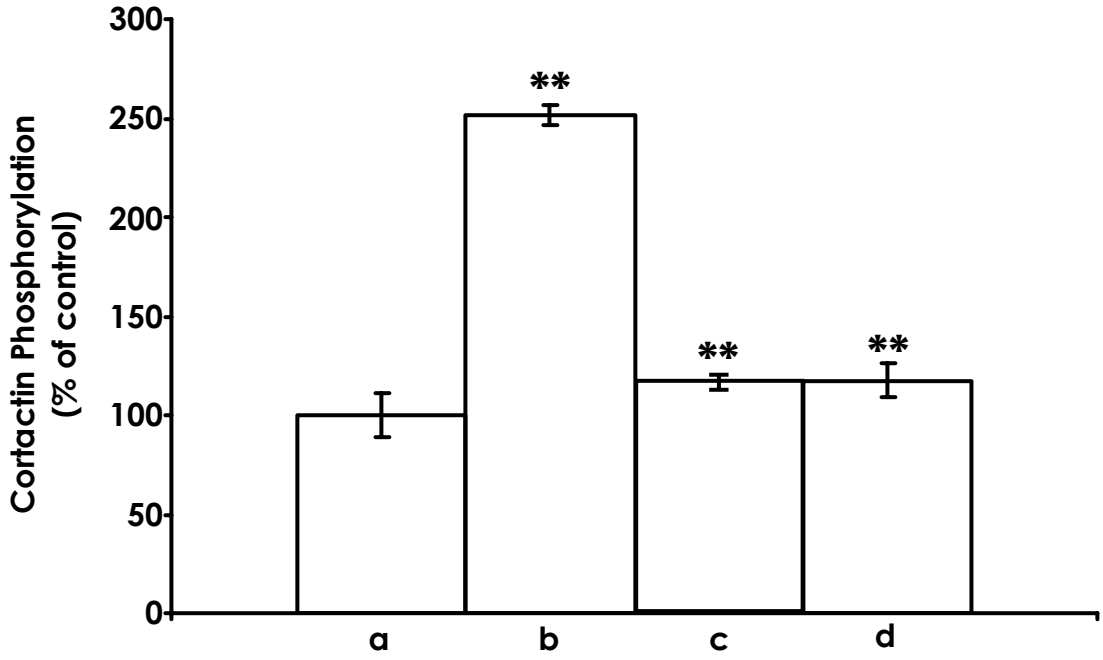
Cortactin Phosphorylation
(% of control)
300
250
200
150
100
50
0
**
**
**
a
b
c
d

B

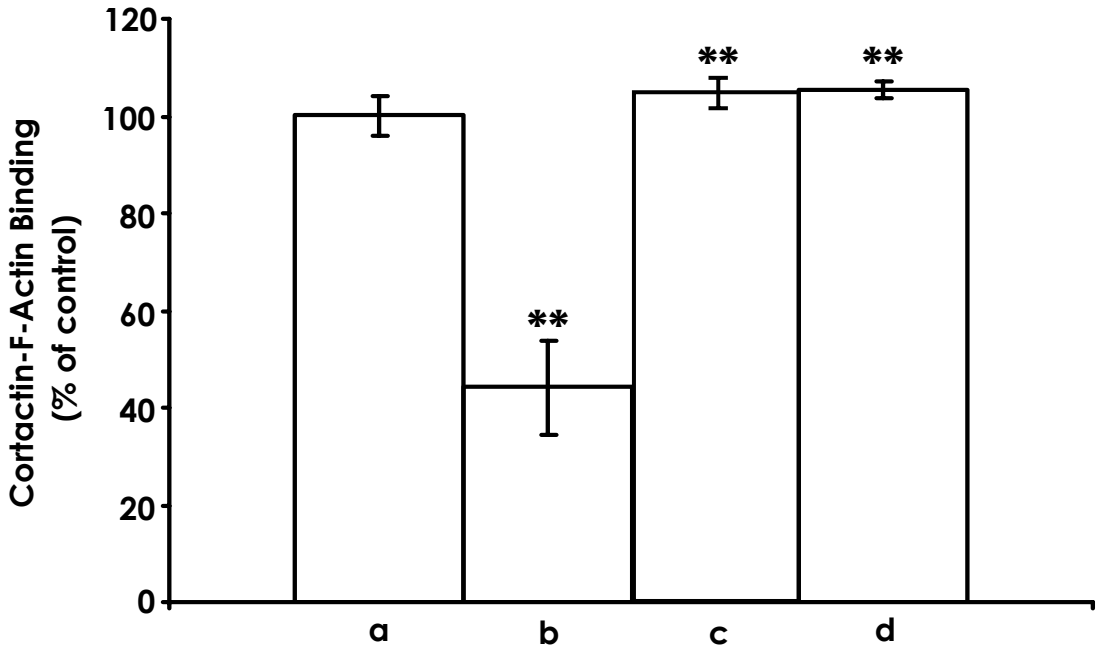
Cortactin-F-Actin Binding
(% of control)
120
100
80
60
40
20
0
**
**
**
a
b
c
d

A

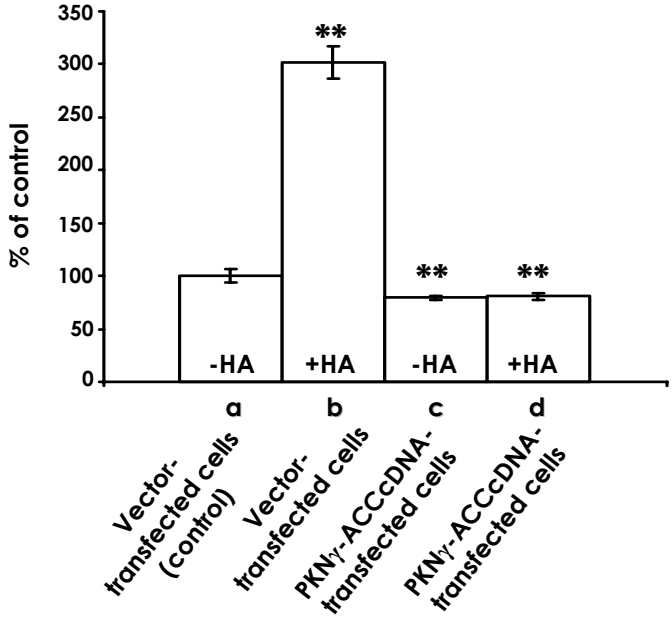
% of control
350
300
250
200
150
100
50
0
**
**
**
-HA
+HA
-HA
+HA
a
b
c
d
Vector-transfected cells (control)
Vector-transfected cells
PKNγ-ACCcDNA-transfected cells
PKNγ-ACCcDNA-transfected cells

B-(I)

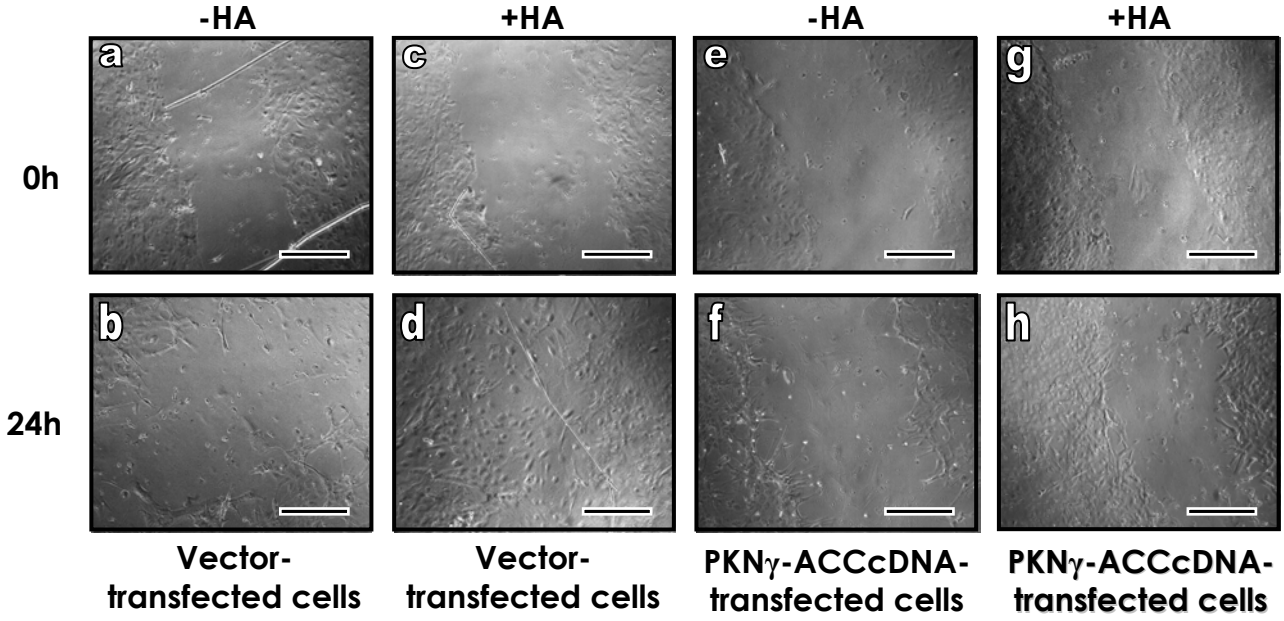
-HA
+HA
-HA
+HA
0h
24h
a
c
e
g
b
d
f
h
Vector-transfected cells
Vector-transfected cells
PKNγ-ACCcDNA-transfected cells
PKNγ-ACCcDNA-transfected cells

B-(II)

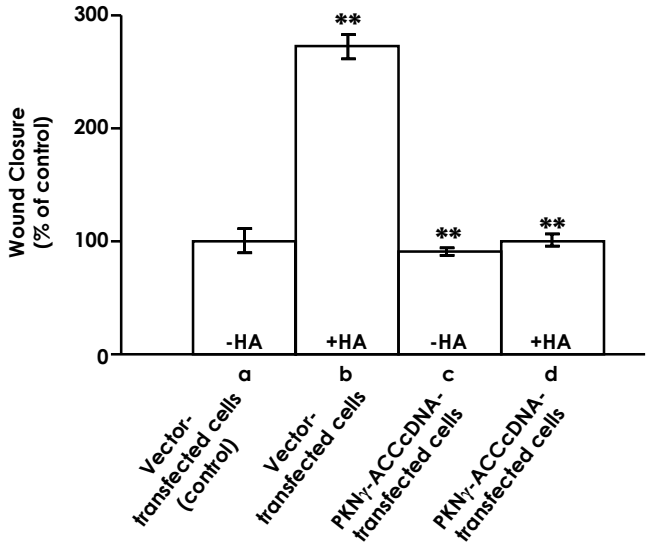
Wound Closure (% of control)
300
200
100
0
**
**
**
-HA
+HA
-HA
+HA
a
b
c
d
Vector-transfected cells (control)
Vector-transfected cells
PKNγ-ACCcDNA-transfected cells
PKNγ-ACCcDNA-transfected cells

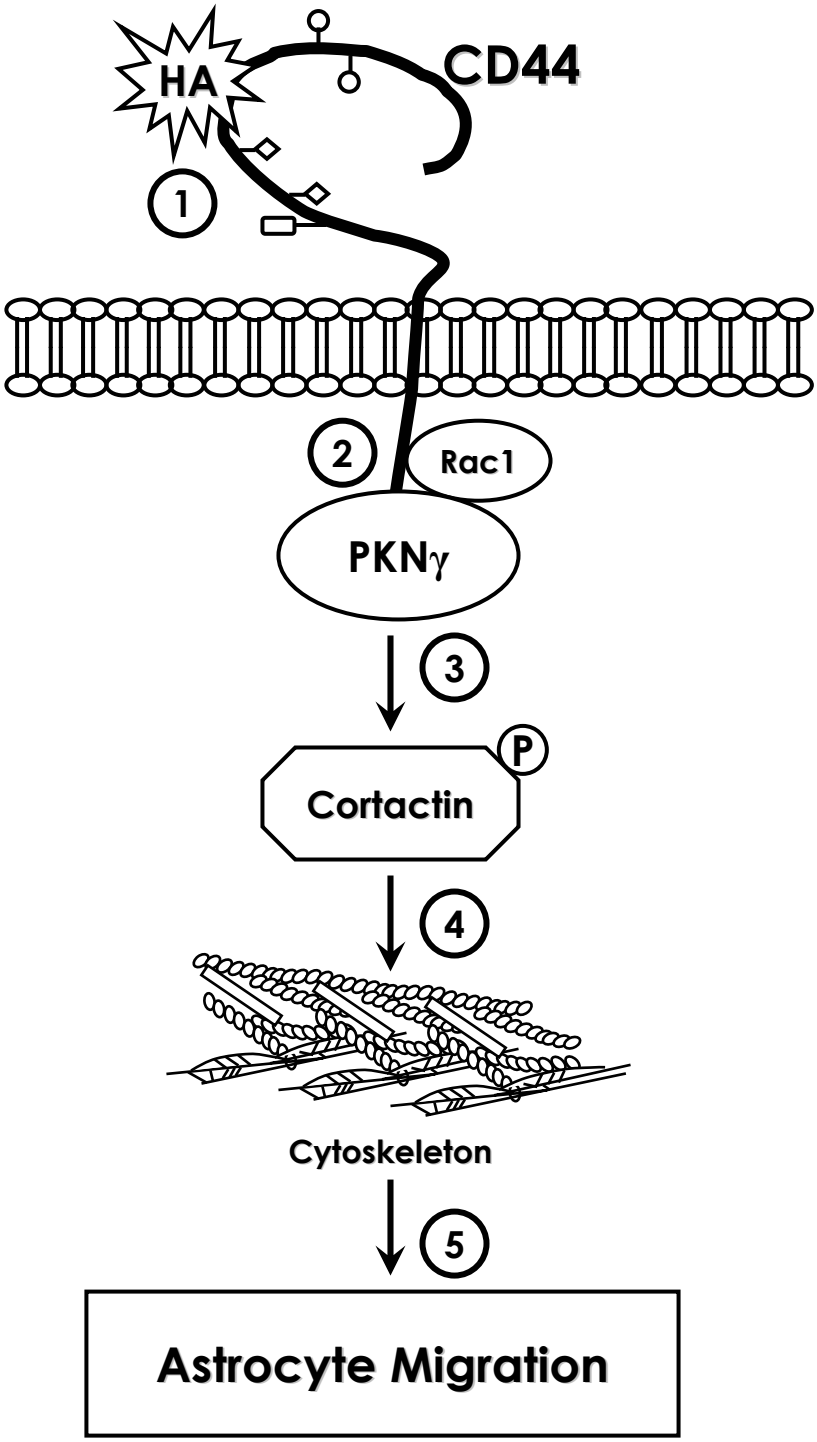
HA
CD44
1
2
Rac1
PKNγ
3
P
Cortactin
4
Cytoskeleton
5
Astrocyte Migration